Structural Insights into Retinal Guanylylcyclase-GCAP-2 Interaction Determined by Cross-Linking and Mass Spectrometry

ARTICLE *in* BIOCHEMISTRY · MAY 2012

Impact Factor: 3.02 · DOI: 10.1021/bi300064v · Source: PubMed

7 AUTHORS, INCLUDING:

Bjoern E S Olausson
Martin Luther University Halle-Wittenberg
5 PUBLICATIONS **62** CITATIONS
SEE PROFILE

Knut Kölbel
University of Antwerp
11 PUBLICATIONS **112** CITATIONS
SEE PROFILE

Christian Lange
Scil Proteins Gmbh
33 PUBLICATIONS **883** CITATIONS
SEE PROFILE

Andrea Sinz
Martin Luther University Halle-Wittenberg
124 PUBLICATIONS **2,437** CITATIONS
SEE PROFILE

BIOCHEMISTRY
including biophysical chemistry & molecular biology

Article

pubs.acs.org/biochemistry

Structural Insights into Retinal Guanylylcyclase−GCAP-2 Interaction Determined by Cross-Linking and Mass Spectrometry

Jens Pettelkau,[†] Thomas Schröder,[‡] Christian H. Ihling,[†] Björn E. S. Olausson,[†] Knut Kölbel,[†] Christian Lange,[‡] and Andrea Sinz*[,†]

[†]Department of Pharmaceutical Chemistry and Bioanalytics, Institute of Pharmacy, Martin-Luther University Halle-Wittenberg, Wolfgang-Langenbeck-Straße 4, D-06120 Halle (Saale), Germany

[‡]Department of Technical Biochemistry, Institute of Biochemistry and Biotechnology, Martin-Luther University Halle-Wittenberg, Kurt-Mothes-Straße 3, D-06120 Halle (Saale), Germany

Supporting Information

ABSTRACT: The retinal guanylylcyclases ROS-GC 1 and 2 are regulated via the intracellular site by guanylylcyclase-activating proteins (GCAPs). The mechanisms of how GCAPs activate their target proteins remain elusive as exclusively structures of nonactivating calcium-bound GCAP-1 and -2 are available. In this work, we apply a combination of chemical cross-linking with amine-reactive cross-linkers and photoaffinity labeling followed by a mass spectrometric analysis of the created cross-linked products to study the interaction between N-terminally myristoylated GCAP-2 and a peptide derived from the catalytic domain of full-length ROS-GC 1. In our studies, only a few cross-linked products were obtained for calcium-bound GCAP-2, pointing to a well-defined structure of the GCAP-2−GC peptide complex. A much larger number of cross-links were detected in the absence of calcium, indicating a high flexibility of calcium-free GCAP-2 in the complex with the GC peptide. On the basis of the distance constraints imposed by the cross-links, we were able to create a structural model of the calcium-loaded complex between myristoylated GCAP-2 and the GC peptide.

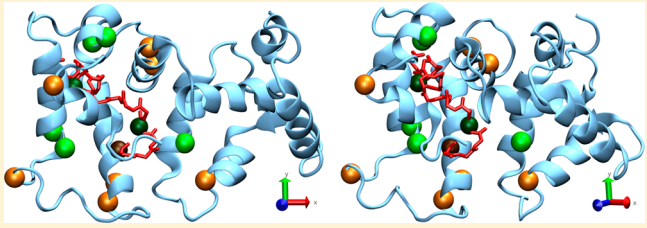

Two isoforms of retinal guanylylcyclase (ROS-GC 1 and 2, also known as GC-E and -F or retGC-1 and -2), localized in photoreceptor cells are responsible for the synthesis of cGMP, the second messenger in phototransduction.[1−4] ROS-GC 1 and 2 are regulated via the intracellular site by calcium-binding proteins, which are termed guanylylcyclase-activating proteins (GCAPs). A number of additional membrane-bound guanylylcyclases are regulated by extracellular ligands, such as the natriuretic peptide.[5,6] GCAPs belong to the neuronal calcium sensor (NCS) family within the superfamily of calmodulin-like four EF-hand calcium-binding proteins. A common feature of all NCS proteins is the dysfunctional EF-hand 1 caused by a conserved proline residue in its core loop, making it impossible for this EF-hand to bind calcium.[7,8] The three remaining EF-hands of GCAP-2 are able to bind calcium; at low calcium concentrations, they can also be occupied by Mg^{2+}.[9,10] Like many calcium sensor proteins, GCAPs are N-terminally myristoylated.[11] The exact function of the myristoylation is not fully understood and is controversially discussed.[12−14] Three GCAP isoforms (GCAP-1−3) were identified in mammalian photoreceptor cells and activate both isoforms of retinal guanylylcyclase, ROS-GC 1 and 2, at free calcium concentrations below 200 nM.[15−19] Furthermore, GCAP-2 inhibits guanylylcyclase activity at the high calcium levels present in dark-adapted photoreceptor cells.[15,20] The GCAP-mediated calcium-dependent regulation of ROS-GC 1 and 2 plays a central role in shaping the photoreceptor light response and in light adaptation.[21−25]

The mechanisms of how GCAPs activate their target protein remain elusive as only structures of nonactivating calcium-bound GCAP-1[13] and -2[26] are available; no high-resolution structures of ROS-GC 1 and 2 have been published. In fact, ROS-GC 1 and 2 are catalytically active as homodimers, which rely on a correct orientation of the active site formed by both subunits.[27,28] As a consequence, GCAP dimerization followed by dimerization of ROS-GC is conceivable, as has been proposed for GCAP-2, but not for GCAP-1.[29] Because of the abundance of different domains and regulating proteins, several regulatory binding sites have been postulated for ROS-GC. Further investigations indicate the presence of three different regulatory binding sites for GCAP-1 in the juxtamembrane domain,[30] the kinase homology domain,[31] and the catalytic domain[32] of ROS-GC. GCAP-2 is supposed to bind more tightly to the GCAP-1 binding site in the catalytic domain of ROS-GC than GCAP-1 itself.[32] Another GCAP-2 binding site was identified in the catalytic domain next to the C-terminal extension, which is not a GCAP-1 binding site, allowing a functional mapping of ROS-GC 1. Apparently, GCAP-2 transmits the calcium signal rather from the C-terminal side, while GCAP-1 exerts its function more from the distant N-terminal side.[33]

Received: January 16, 2012
Revised: March 31, 2012
Published: May 25, 2012

dx.doi.org/10.1021/bi300064v | *Biochemistry* 2012, 51, 4932−4949

Genetic disorders in GCAP genes or parts of the regulatory regions in ROS-GC genes result in different malfunctions. Especially a variant of GCAP-1, Y99C, leads to a reduced calcium sensitivity and a progression of autosomal dominant cone dystrophy.[34,35] There are also other known mutations in GCAP-2 genes, such as a codon exchange from GGA to AGA resulting in a G157R mutation, which is associated with retinitis pigmentosa.[36] For the design of novel drugs, a detailed molecular knowledge of the formation of the complex between GCAP-2 and ROS-GC 1 is crucial. Therefore, we performed cross-linking experiments between N-terminally myristoylated GCAP-2 and peptides containing the predicted GCAP-2 binding side comprising amino acids 965−981[33] in the catalytic domain of full-length ROS-GC 1.

Chemical cross-linking relies on the introduction of a covalent bond between functional groups of specific amino acids between different interaction partners by a chemical reagent for the elucidation of interfaces in protein complexes.[37−45] After the cross-linking reaction, the proteins of interest are usually enzymatically digested, and the resulting peptide mixtures are analyzed by high-resolution mass spectrometry (MS).[40] We have recently shown for N-terminal (LN) domains of laminins that even a few distance constraints imposed by chemical cross-links and disulfide bonds, i.e., "natural" cross-links, are sufficient for deriving a valid structural model[46] that closely resembles the structure obtained by X-ray crystallography.[47] So far, the largest protein complex analyzed in depth by chemical cross-linking and MS is the 15-subunit 670 kDa complex of RNA polymerase II (Pol II) with transcription initiation factor TFIIF.[48] Despite its straightforwardness, the greatest challenge of the cross-linking approach is posed by the high level of complexity of the created peptide mixtures requiring high-resolution MS techniques for analysis of the cross-linked products.

In a previous study, we have demonstrated[49] that a combination of chemical cross-linking with amine-reactive cross-linkers and photoaffinity labeling yields complementary results and is thus advantageous for deriving detailed models of protein complexes. In this work, we apply both complementary cross-linking strategies to study the interaction between N-terminally myristoylated GCAP-2 and a ROS-GC 1 peptide derived from the catalytic domain of full-length ROS-GC in the presence and absence of calcium.

EXPERIMENTAL PROCEDURES

Materials. Recombinant N-terminally myristoylated bovine GCAP-2 was produced according to an existing protocol.[14] A peptide comprising amino acids 965−981 of full-length ROS-GC 1 was synthesized by Dr. Rothemund (IZKF Leipzig). In the following, we will refer to this peptide simply as GC peptide. Both photoleucine-labeled GC peptides shown in Scheme 1 were custom synthesized (ThermoFisher Scientific, Ulm, Germany). BS^2G [bis(sulfosuccinimidyl)glutarate] was obtained from ThermoFisher Scientific (Rockford, IL). HEPES [4-(2-hydroxyethyl)-1-piperazineethanesulfonic acid], ammonium bicarbonate, DMSO (dimethyl sulfoxide), $CaCl_2$, and EGTA (ethylene glycol tetraacetic acid) were purchased from Sigma-Aldrich (Steinheim, Germany). Laemmli sample buffer was purchased from Bio-Rad (Munich, Germany). Trypsin (bovine) was purchased from Roche (Mannheim, Germany); trypsin (porcine) was obtained from Promega (Madison, WI), and endoproteinase GluC was purchased from Roche. Nano-HPLC solvents were purchased from VWR (Darmstadt, Germany). Milli-Q water was produced by a TKA Pacific apparatus with an X-CAD dispenser from Thermo Electron LED GmbH (part of ThermoFisher Scientific, Niederelbert, Germany).

Cross-Linking Reactions. For cross-linking reactions with the amine-reactive *N*-hydroxysuccinimide (NHS) ester cross-linker BS^2G, a stock solution (19 μM) of bovine GCAP-2 was diluted to give a final protein concentration of 10 μM in 20 mM HEPES (pH 7.5). The mixture was incubated at room temperature for 10 min after the addition of $CaCl_2$ (final concentration of 1 mM; calcium-loaded GCAP-2) or EGTA (pH 7.5) (final concentration of 10 mM; calcium-free GCAP-2). An aqueous stock solution of GC peptide (221 μM) was added to each sample (final concentration of 31 μM), and the mixtures were incubated at room temperature for 30 min. The cross-linking reactions were initiated by adding a freshly prepared solution of nondeuterated (D_0) and 4-fold deuterated (D_4) BS^2G (1:1) in DMSO to give a final cross-linker concentration of 1 mM (100-fold molar excess over GCAP-2 concentration). As a control sample, the same amount of DMSO was added to the peptide/protein mixture. Reaction mixtures were incubated at room temperature, and aliquots were taken after 30 and 60 min. The cross-linking reactions were quenched by adding ammonium bicarbonate (final concentration of 20 mM) and used immediately or stored at −20 °C before SDS−PAGE and MALDI-TOF-MS analysis.

For photo-cross-linking reactions of GCAP-2 with photo-Leu-modified GC peptides (Scheme 1), a stock solution of bovine GCAP-2 (19 μM) was diluted to give a final protein concentration of 10 μM in 20 mM HEPES (pH 7.5). GCAP-2 was incubated at room temperature for 10 min after adding $CaCl_2$ (final concentration of 1 mM; calcium-loaded GCAP-2) or EGTA (pH 7.5) (final concentration of 10 mM; calcium-free GCAP-2). An aqueous stock solution of GC photopeptide 1 (175 μM) or GC photopeptide 2 (115 μM) was added to each sample to give a final peptide concentration of 10 μM. The mixtures were incubated in the dark at room temperature for 30 min. The photo-cross-linking reactions between GCAP-2 and GC photopeptides were performed by irradiation with UV-A light (365 nm) on ice. Aliquots were taken at irradiation energies of 4000 and 8000 mJ/cm^2. One aliquot without irradiation served as control sample. Samples were used immediately or stored at −20 °C before SDS−PAGE and MALDI-TOF-MS analysis.

SDS−PAGE and Enzymatic Proteolysis. After separation of the cross-linking reaction mixtures by one-dimensional gel electrophoresis (SDS−PAGE, 20 μL of the reaction mixture per lane; 15% resolving gel; Coomassie Blue Silver staining[50]). BS^2G-cross-linked samples were additionally treated in the following manner: 25 μL of the solution was desalted using Amicon filtration units (Millipore Corp., Billerica, MA) (cutoff of 10 kDa, 0.5 mL) before the cross-linking reaction mixtures were separared on gradient gels (4 to 20%, ThermoFisher Scientific; Coomassie Blue Silver staining[50]). Bands of interest were excised; the proteins contained in the bands were reduced with DTT (dithiothreitol) and carbamidomethylated with IAA (iodoacetamide). In-gel digestion was performed by simultaneous digestion with trypsin (cleaving on the C-terminal side of Arg and Lys) and endoproteinase GluC (cleaving on the C-terminal side of Glu and Asp) according to existing protocols.[51,52] Depending on the size of the gel bands and staining intensities, different amounts of the enzyme solution (in 25 mM NH_4HCO_3) were added [~1:15 to 1:20 (w/w) enzyme:protein ratio], and samples were incubated at 30 °C overnight. Proteolytic peptides were extracted, and extracts of three bands resulting from identical reaction mixtures were combined. Samples were used immediately or stored at −20 °C before nano-HPLC/nano-ESI-LTQ-Orbitrap MS analysis.

dx.doi.org/10.1021/bi300064v | *Biochemistry* 2012, 51, 4932−4949

Scheme 1. Amino Acid Sequence of Bovine GCAP-2 and Locations of GC Peptide in ROS-GC 1[a]

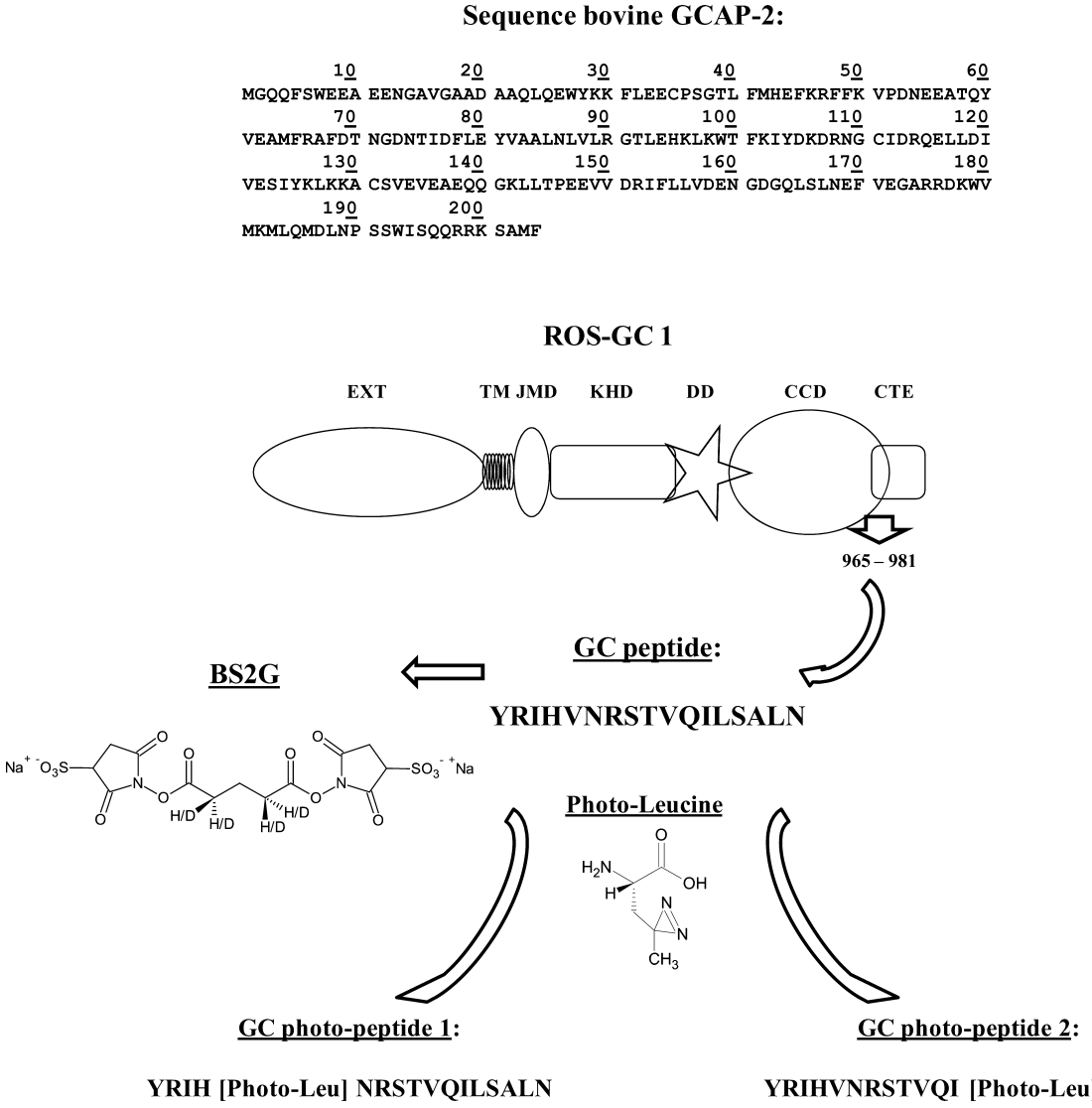

[a]Workflow for identifying sites of interaction between GCAP-2 and GC peptide by chemical cross-linking with BS^2G and photoaffinity labeling using photo-Leu-modified GC peptides. ROS-GC 1 domains are denoted as EXT: extramembrane domain, TM: transmembrane domain, JMD: juxtamembrane domain, KHD: kinase homology domain, DD: dimerization domain, CCD: catalytic cyclase domain, CTE: C-terminal domain.

MALDI-TOF Mass Spectrometry. Ten microliters of each cross-linking reaction mixture was desalted with C4 ZipTips (Millipore Corp.). The samples were spotted onto a steel target using the thin-layer method: 0.3 μL of a saturated solution of sinapinic acid in ethanol was spotted to form a thin layer. One microliter of a desalted sample solution was premixed with 1 μL of a saturated solution of sinapinic acid in a 33% (v/v) ACN/0.1% (v/v) TFA mixture in water. One microliter of this solution was spotted onto the prepared thin layer. MALDI-TOF-MS measurements were conducted on an Ultraflex III MALDI-TOF/TOF mass spectrometer (Bruker Daltonik, Bremen, Germany). Spectra were recorded in the m/z range of 5000−100000 in the linear and positive ionization modes; 2000 spectra were added to one mass spectrum. Acquisition and analysis of data were performed with FlexControl (version 3.3) and FlexAnalysis (version 3.3).

Off-Line Nano-ESI Mass Spectrometry. Fifteen microliters of each cross-linking reaction mixture was desalted with C4 ZipTips (Millipore Corp.). Off-line nano-ESI-MS measurements for detecting intact cross-linked products between GCAP-2 and GC peptides were conducted on an LTQ-Orbitrap XL mass spectrometer (ThermoFisher Scientific, Bremen, Germany) with a nano-ESI source (Proxeon, Odense, Denmark). For off-line nano-ESI-MS measurements, borosilicate emitters (ES380, Proxeon/ThermoFisher Scientific) were filled with 5 μL of sample solution. Mass spectra were recorded in the orbitrap over variable m/z ranges at a resolution of 100000 at m/z 400. Acquisition and analysis of data were performed with Xcalibur version 2.0.7 (ThermoFisher Scientific). Mass spectra were deconvoluted ($[M + H]^+$) with the Xtract software in the Qual Browser.

Nano-HPLC/Nano-ESI-LTQ-Orbitrap Mass Spectrometry. Separation of enzymatic digestion mixtures was conducted on a nano-HPLC system (Ultimate, Dionex Corp., Idstein, Germany) equipped with a Famos autosampler and a Switchos device (Dionex). First, peptides were loaded onto the precolumn (Acclaim PepMap, 100 μm × 20 mm, 5 μm, 100 Å) and washed with 0.1% (v/v) TFA in water for 15 min at a flow rate of 20 μL/min. Afterward, peptides were eluted from the precolumn and separated on a C18 reversed

dx.doi.org/10.1021/bi300064v | *Biochemistry* 2012, 51, 4932−4949

phase separation column (Acclaim PepMap, 75 μm × 250 mm, 3 μm, 100 Å, Dionex) using three different gradients: gradients 1 and 2 ranging from a 95% water/5% ACN/0.1% FA mixture to a 60% water/40% ACN/0.09% FA mixture over 90 and 45 min, respectively (an 80% ACN/20% water/0.08% FA mixture was used after finishing the gradient to elute highly hydrophobic peptides), and gradient 3 ranging from a 95% water/5% ACN/0.1% FA mixture to a 76% water/24% ACN/0.1% FA mixture over 120 min to a 60% water/40% ACN/0.09% FA mixture. Afterward, a mixture of 10% water, 80% ACN, 10% TFE (trifluoroethanol), and 0.08% FA was used to additionally elute highly hydrophobic peptides.

The nano-HPLC system was coupled to a nano-ESI source (Proxeon) of an LTQ-Orbitrap XL mass spectrometer (ThermoFisher Scientific, Bremen, Germany). MS data were acquired continuously during the gradient between 78 and 195 min, excluding the washing step. Each full MS scan was acquired in the orbitrap (m/z 350−2000, resolution of 60000). The five most intense signals of each full MS scan were automatically selected for collision-induced dissociation (CID) in the linear ion trap (LTQ) (isolation window of 2 Th, normalized collision energy of 35), and fragment ions were analyzed in the LTQ. Dynamic exclusion (window of −1/+2 Th, duration of 120 s) was used to detect and fragment less abundant signals. Acquisition of data was controlled via Xcalibur version 2.0.7 (ThermoFisher) in combination with DCMS link version 2.0 (Dionex).

Identification of Cross-Linked Products. Analysis and identification of cross-linked products were performed with GPMAW (General Protein Mass Analysis for Windows, versions 8.1−9.0, Lighthouse Data, Odense, Denmark) and the in-house software StavroX.[53] With GPMAW, acquired mass lists were matched with theoretical cross-linked products. Fragment ion mass spectra of potential cross-linked products were manually assigned. StavroX was used for automatic comparison of MS and MS/MS data from Mascot generic files (mgf). Potential cross-links were manually evaluated. For comparison of masses from cross-linking experiments with BS^2G, a maximal mass deviation of 6 ppm between theoretical and experimental precursor ion mass and a signal-to-noise ratio (S/N) of ≥2 were accepted, while for photoaffinity labeling experiments with GC photopeptides, a maximal mass deviation of 5 ppm was allowed. Lys, Ser, Tyr, Thr, and N-termini were considered as potential cross-linking sites for the NHS ester BS^2G.[54] For analyzing cross-linked products with GC photopeptides, Ala, Asp, Glu, Gly, Ile, Leu, Lys, Met, Phe, Ser, Thr, Tyr, and Val were considered as potential reaction sites of diazirines. As the carbene intermediate is highly reactive, diazirines will react with a large number of amino acids. When analyzing cross-linked products, we took into account that also neighboring amino acids might have reacted. Additionally, carbamidomethylation of Cys and oxidation of Met were taken into account as potential modifications as well as up to a total of eight missed cleavage sites (analysis with GPMAW) or three missed cleavage sites for each amino acid Lys, Arg, Glu, Asp (analysis with StavroX).

Circular Dichroism (CD) Measurements. Solutions (146 μM) of GC peptide in H_2O and 60% (v/v) TFE were prepared to give final TFE concentrations of 0−60% (v/v). If desired, a 1 M stock solution (pH 7.5) of K_2HPO_4/KH_2PO_4 was added to give a final concentration of 25 μM. Far UV-CD spectra of the solutions were recorded in a 0.5 mm fused silica cuvette on a J-810 spectropolarimeter (Jasco, Groß-Umstadt, Germany) at 4 °C from 260 to 180 nm with scan rates of 20 nm/min, data pitches of 0.1 nm, response times of 4 s, and bandwidths of 1 nm. Depending on the signal intensity, 10−20 single spectra were averaged. The raw spectra were normalized depending on the peptide bond concentration ($[\Theta]_{MRW}$). No smoothing procedure was applied.

Molecular Modeling. The GC peptide was manually placed into the GCAP-2 NMR structure (PDB entry 1JBA). PSIPRED (http://bioinf.cs.ucl.ac.uk/psipred) was used to predict the secondary structure of the GC peptide. A 20 ns all-atom molecular dynamics (MD) simulation with explicit water was conducted using NAMD[55] (CVS-2011-11-16) with the CHARMM27[56] all-atom force field. The protein−peptide complex was neutralized and solvated in 0.15 M $CaCl_2$ using the TIP3P water model. Calcium ions trapped in an EF-hand motif were preserved. Periodic boundary conditions were set up as a square box with a side length of 78 Å. Long-range electrostatic interactions were calculated using the smooth particle mesh Ewald[57] summation technique with a grid spacing of 1 Å for the fast Fourier transformation. Real space electrostatics were truncated at 16 Å with switching of nonbonded interactions starting at 15 Å. Bonds involving hydrogens were treated with the SHAKE[58] algorithm allowing the simulation to run with a time step of 2 fs. The system was minimized for 10000 steps and equilibrated using a canonical ensemble (NVT) at 303 K for 1 ns. The pressure and temperature were kept constant (1 bar and 303 K, respectively; isothermal−isobaric *NPT* ensemble) for the production run using the Nose−Hoover−Langevin pressure piston control.[59,60] During the first 10 ns of the production run, distance constraints were applied to selected amino acids. The lower boundary was set to 0 Å with a lower wall of 1 Å for all cross-links. The upper boundary was set to 19 Å with an upper limit of 18 Å for the amine-reactive cross-links. For the photoreactive cross-links, an upper boundary of 10 Å with an upper limit of 9 Å was assumed. The maximal biasing force was increased in a stepwise manner (20, 50, 80, 100, and 200 kcal/mol) in 1 ns intervals and run for 6 ns at the highest setting.

RESULTS

Analytical Strategy of Chemical Cross-Linking. Cross-linking reactions between GCAP-2 and a GC peptide containing the predicted GCAP-2 binding side comprising amino acids 965−981[33] in the catalytic domain of ROS-GC 1 (Scheme 1) were conducted as described in Experimental Procedures. The amine-reactive, homobifunctional cross-linker BS^2G and photoreactive derivatives of the GC peptide, into which the diazirine-containing photoleucine had been incorporated at specific positions, were used for cross-linking experiments. BS^2G, as a homobifunctional cross-linker, carries two identical amine-reactive sites (Scheme 1). It reacts with ε-amino groups of lysine side chains and the N-terminus of a protein or a peptide to form an amide bond, while *N*-hydroxysulfosuccinimide and water are released. Reactions with hydroxyl groups of Ser, Thr, or Tyr side chains lead to the formation of ester bonds.[54,61] Cross-linked species are identified by their typical isotope pattern (4 amu mass difference) in the mass spectra, because of the use of non-deuterated and 4-fold deuterated BS^2G, and mass increases of 96.021 (BS^2G-D_0) and 100.052 Da (BS^2G-D_4) in the combined peptide masses. Peptides that are modified by a partially hydrolyzed cross-linker exhibit mass increases of 114.032 (BS^2G-D_0) and 118.063 Da (BS^2G-D_4), respectively.

The GC peptide derived from the postulated GCAP-2 binding region[33] was modified at two positions (Val-5 and Leu-13) with the photoreactive amino acid photo-Leu (Scheme 1). Photo-Leu is an artificial amino acid carrying a photoreactive diazirine group.[62] Upon activation by UV-A light, diazirines lose nitrogen and thus form a multireactive carbene, which reacts nonspecifically with

various amino acid side chains. Photo-cross-linked species are readily identified by the loss of nitrogen, resulting in a mass difference of 28.006 Da.

In previous studies, we have shown that cross-linking experiments with amine-reactive NHS esters and photo-amino acids yield complementary results in structural analyses of proteins.[49] NHS esters bridge distances depending on the length of the spacer chain and, as such, detect more flexible interaction regions within the proteins, while photoreactive amino acids identify spatially close or even directly interacting surfaces in the interaction partners.

Analysis of Intact GCAP-2−GC Peptide Complexes. After the cross-linking reactions, SDS−PAGE (Figure S1, Supporting Information), off-line nano-ESI-Orbitrap MS (Figure 1), and MALDI-TOF-MS (Figure S2, Supporting Information) were performed to verify whether a covalent complex had been created between GCAP-2 and the respective GC peptide. SDS−PAGE showed bands of a 1:1 complex between GCAP-2 and GC peptides after the cross-linking reaction with BS^2G in the presence and absence of calcium. In photoaffinity labeling experiments using photo-Leu peptides, it was hardly possible to identify clear signals for 1:1 complexes in the presence of calcium because of the existence of the different calcium-loaded states of GCAP-2. In the absence of calcium, a weak band of the 1:1 complex was visible (Figure S1, Supporting Information). To confirm the formation of GCAP-2−GC peptide complexes, off-line nano-ESI and MALDI-TOF-MS measurements were performed giving a much clearer picture of the stoichiometries of the GCAP-2−GC peptide complexes, the degree of cross-linker modification, and the cross-linking efficiency.

High-resolution off-line nano-ESI-LTQ-Orbitrap-MS measurements of intact GCAP-2−GC peptide complexes unambiguously demonstrated the presence of cross-linked complexes both for the amine-reactive cross-linker BS^2G (Figure 1A) and for GC photopeptides (Figure 1B,C). As the orbitrap technique yields data with both high mass accuacy and excellent mass resolution, we were able to unambiguously determine the number of cross-linker modifications in the GCAP-2−GC peptide complexes.

In the MALDI-TOF mass spectra, highly intense signals of singly and doubly charged BS^2G-modified GCAP-2 were observed in addition to a smaller signal corresponding to a 1:1 complex between GCAP-2 and GC peptide (Figure S2, Supporting Information). The mass of GCAP-2 slightly increased at reaction times between 30 and 60 min, probably because of a stronger modification with partially hydrolyzed and intramolecularly bound BS^2G cross-linker, while the mass of the GCAP-2−GC peptide (1:1) complex was essentially identical (data not shown). MALDI-TOF-MS measurements of the photo-cross-linking mixtures with each of the two photo-Leu-modified GC peptides showed a strong signal of intact GCAP-2 with a small signal in the mass region of the GCAP-2−GC peptide (1:1) complex. Mass spectra of nonirradiated and irradiated (irradiation energies of 4000 and 8000 mJ/cm^2) samples were nearly identical (data not shown), indicating that the photoreaction was already induced by ambient light.

Identification of Contact Sites between GCAP-2 and GC Peptides by Amine-Reactive Cross-Linking. So far, no structural information is available for the complex between GCAP-2 and ROS-GC. The GC peptide used for this work had been postulated as a potential GCAP-2 binding site.[33] To verify this binding site and, moreover, to gain insight into the mechanisms underlying the interaction between GCAP-2 and ROS-GC, we performed cross-linking experiments, first with the homobifunctional amine-reactive cross-linker BS^2G that possesses a spacer length of ∼7.8 Å.

After the cross-linking reaction, the cross-linking reaction mixtures were separated by one-dimensional gel electrophoresis (SDS−PAGE) with the aim of excising the bands of cross-linked complexes from the gel and subjecting them to in-gel digestion, yet as SDS−PAGE hardly revealed a distinct band of a 1:1 complex between GCAP-2 and the GC peptide, the whole smeared band was cut out and divided into different partitions. Because there are only a few cleavage sites for trypsin in GCAP-2 (Scheme 1), we performed digestions with a combination of the proteases trypsin (cleaving to the C-terminal side of Lys and Arg) and GluC (cleaving to the C-terminal side of Glu and also Asp) to create fragments of cross-linked products in the optimal mass range of <4000 Da. Peptide mixtures were subsequently separated by nano-HPLC and analyzed by high-resolution nano-ESI mass spectrometry.

First, we analyzed the peptide mixtures from the different excised gel band segments (vide supra) to verify the presence of each of the binding partners (GC peptide and GCAP-2) in the gel regions of interest. Indeed, we were able to identify the GC peptide in gel bands representing potential complexes from reaction mixtures both with and without calcium, indicating that a complex between GCAP-2 and GC peptide had been created during the cross-linking reaction (Table S1, Supporting Information). GC peptide fragments corresponding to amino acids 8−17 ($[M + 2H]^{2+}$ at m/z 522.806) and amino acids 3−13 ($[M + 2H]^{2+}$ at m/z 832.486) were identified from cross-linking reaction mixtures with calcium (Table S1, Supporting Information). In samples without calcium, a signal at m/z 522.806 of a doubly charged species was observed corresponding to amino acids 8−17 of GC peptide (Table S1, Supporting Information). Thus, we were encouraged to conduct a more detailed analysis of the excised gel bands with respect to intra- and intermolecular cross-linked products within GCAP-2 and between GCAP-2 and GC peptide, respectively. All cross-linked product candidates were verified via MS/MS experiments.

In the presence of calcium, several intramolecular cross-links were identified within N-terminally myristoylated GCAP-2 (Table 1), all of which are in agreement with the published NMR structure of nonmyristoylated GCAP-2 (Figure S3, Supplemetary Information).[26] In particular, the C-terminal part of GCAP-2, which is not resolved in the NMR structure, seems to be very flexible as indicated by the numerous intramolecular cross-links within GCAP-2 in this region. As such, Lys-200 in the C-terminal region of GCAP-2 was found to be connected with lysines at positions 29, 30, 46, 50, 96, 126, 128, 129, 142, and 178. Several cross-linked products (Table 2) point to interactions between nine amino acids of GCAP-2 and the N-terminal Tyr of the GC peptide. As a typical example for the analysis of a cross-linked product, MS and MS/MS data of a cross-linked product between amino acids Lys-129−Glu-136 of GCAP-2 and Tyr-1 and Arg-2 of GC peptide are shown in Figure 2. Except for one cross-link between Lys-29 of GCAP-2 and the N-terminal Tyr of the GC peptide, all cross-links fall within the range of the 25 Å maximal Cα−Cα distance that BS^2G is able to bridge.[48,49] On the basis of these connection points, we aimed to construct a viable structure of the GCAP-2−GC peptide complex using structural modeling (vide infra).

It should also be mentioned in this context that we observed a number of lysines in GCAP-2 that had been modified by a partially hydrolyzed cross-linker (Table S2, Supporting Information).

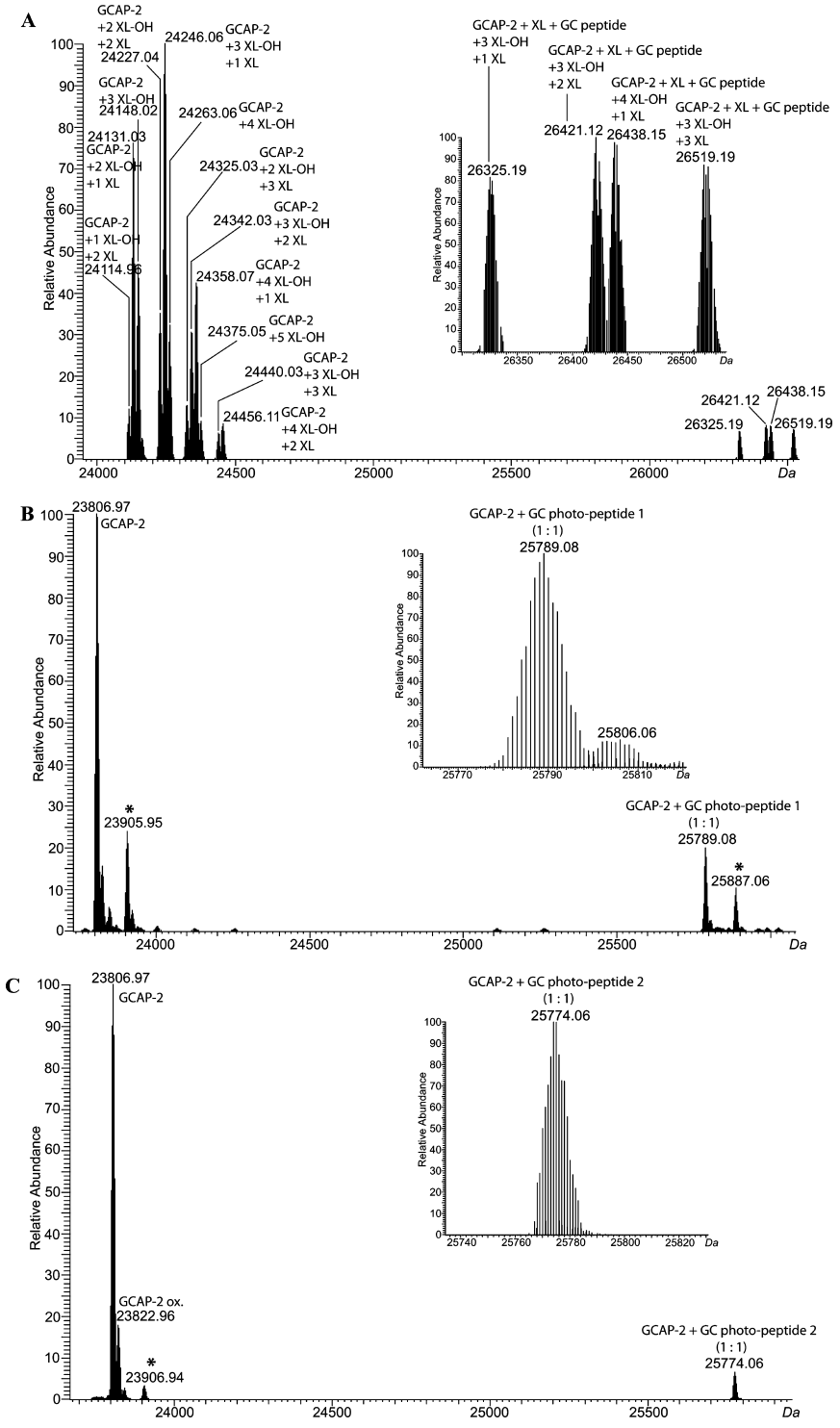

Figure 1. Identification of intact cross-linked complexes via off-line nano-ESI-MS. (A) Deconvoluted mass spectrum ($[M + H]^+$) of cross-linking reaction mixtures between GCAP-2 (10 μM; MW_{av} of 23807.1 Da) and GC peptide (100 μM; MW_{av} of 1983.3 Da) with a 100-fold excess of BS^2G-D_0 and 1 mM Ca^{2+} and a reaction time of 30 min. Abbreviations: XL, intra/intermolecular cross-link (+96 Da); XL-OH, hydrolyzed cross-linker (+114 Da). (B) Deconvoluted mass spectrum ($[M + H]^+$) of the photo-cross-linking reaction mixture between GCAP-2 (10 μM) and GC photopeptide 1 (100 μM; MW_{av} of 2009.3 Da) in the absence of Ca^{2+} (10 mM EGTA; irradiation energy of 4000 mJ/cm^2). (C) Deconvoluted mass spectrum ($[M + H]^+$) of the photo-cross-linking reaction mixture between GCAP-2 (10 μM) and GC photopeptide 2 (100 μM; MW_{av} of 1995.27 Da) in the absence of Ca^{2+} (10 mM EGTA; irradiation energy of 4000 mJ/cm^2). Asterisks denote a potential phosphate adduct of GCAP-2. Data for cross-linked GCAP-2−GC peptide complexes are shown as insets.

These "dead-end" cross-links yield valuable information as they allow us to draw conclusions about the solvent accessibility of specific lysine residues. In this study, we focused on determining the interface between GCAP-2 and GC peptide, yet the obtained dead-end cross-links confirmed that the cross-linking reactions did not disturb GCAP-2's overall three-dimensional (3D) structure.

Analysis of cross-linking samples that had been conducted in the absence of calcium yielded intramolecular cross-linked

dx.doi.org/10.1021/bi300064v | *Biochemistry* 2012, 51, 4932−4949

Table 1. Intramolecular Cross-Links within GCAP-2, Cross-Linked with BS^2G[a]

m/z measured	calcd protonated molecular mass (Da)	charge state	mass deviation (ppm)	cross-linked amino acids in GCAP-2	with (+) or without (−) calcium	amino acids sequences	fragments
535.816	1070.622	2	3.1	K-200 × K-128	+	α ^{200}KSAMF β ^{128}LKK	$b_{\alpha2}$; $b_{\alpha3}$; $b_{\alpha4}$; $y_{\alpha1}$; $y_{\alpha2}$; $y_{\alpha3}$-H_2O; $b_{\beta2}$
566.811	1132.612	2	2.2	K-200 × K-46	+	α ^{200}KSAMF β ^{045}FKR	$b_{\alpha1}$; $b_{\alpha2}$; $b_{\alpha3}$; $b_{\alpha4}$, $y_{\beta2}$-H_2O, or $y_{\beta2}$-NH_3; $y_{\alpha2}$; $y_{\alpha4}$-NH_3; $y_{\beta1}$; $y_{\beta2}$
566.810	1132.612	2	−0.2	K-200 × K-46	−	α ^{200}KSAMF β ^{045}FKR	$b_{\alpha2}$; $b_{\alpha3}$; $b_{\alpha4}$ or $y_{\beta2}$-H_2O; $b_{\alpha4}$-H_2O; $y_{\alpha3}$; $y_{\alpha3}$-H_2O or $y_{\beta1}$; $y_{\alpha2}$; $y_{\alpha3}$; $y_{\alpha4}$-NH_3 or $y_{\alpha4}$-H_2O; $b_{\beta1}$; $y_{\beta2}$
587.340	1173.672	2	1.4	K-29 (alternative K-30) × K-46	+	α ^{027}WYKK β ^{045}FKR	$b_{\alpha2}$; $b_{\alpha3}$; $y_{\alpha2}$; $b_{\beta2}$; $y_{\beta1}$
587.339	1173.672	2	0.0	K-29 (alternative K-30) × K-46	−	α ^{027}WYKK β ^{045}FKR	$b_{\alpha2}$; $b_{\alpha3}$; $y_{\alpha2}$; $y_{\alpha3}$; $b_{\beta2}$; $y_{\beta1}$ or $b_{\alpha2}$; $y_{\beta2}$ alternative K-30: $b_{\alpha3}$-H_2O; $y_{\alpha1}$
604.345	1207.681	2	2.4	K-200 × K-96	+	α ^{200}KSAMF β ^{095}HKLK	$b_{\alpha2}$; $b_{\alpha3}$; $b_{\alpha4}$; $y_{\alpha2}$; $y_{\alpha3}$; $y_{\alpha4}$; $b_{\beta2}$; $b_{\beta3}$-H_2O or $b_{\beta3}$- NH_3; $y_{\beta2}$
644.860	1288.713	2	−0.4	K-200 × K-46	−	α ^{199}RKSAMF β ^{045}FKR	$b_{\alpha2}$; $b_{\alpha3}$; $b_{\alpha4}$; $b_{\alpha5}$-NH_3 or $b_{\alpha5}$-H_2O; $y_{\alpha2}$; $y_{\alpha5}$; $y_{\alpha5}$-H_2O or $b_{\beta2}$; $b_{\beta2}$-NH_3; $y_{\beta2}$; $y_{\beta2}$-NH_3 or $b_{\alpha5}$
653.845	1306.680	2	2.3	K-200 × K-29	+	α ^{200}KSAMF β ^{027}WYKK	$b_{\alpha3}$; $b_{\alpha4}$ or $b_{\beta3}$-H_2O; $y_{\alpha2}$; $b_{\beta2}$; $b_{\beta3}$; $y_{\beta2}$; $y_{\beta2}$-H_2O or $b_{\alpha2}$
661.843	1322.675	2	2.0	K-200 × K-29	+	α ^{200}KSAmF β ^{027}WYKK	$b_{\alpha2}$; $b_{\alpha3}$; $b_{\alpha4}$ or $b_{\beta3}$-H_2O; $y_{\alpha2}$; $y_{\alpha3}$; $y_{\alpha4}$; $b_{\beta3}$; $y_{\beta2}$; $y_{\beta3}$-H_2O
717.406	1433.801	2	2.8	K-126 × K-200	+	α ^{123}SIYKLK β ^{200}KSAMF	$b_{\alpha3}$; $b_{\alpha4}$; $b_{\alpha5}$; $y_{\alpha2}$; $y_{\alpha3}$; $y_{\alpha4}$; $b_{\beta2}$; $b_{\beta3}$; $b_{\beta4}$ or $b_{\alpha5}$-H_2O
752.879	1504.748	2	2.5	K-178 × K-200	+	α ^{177}DKWVMK β ^{200}KSAMF	$b_{\alpha2}$-NH_3; $b_{\alpha4}$; $b_{\alpha5}$; $y_{\alpha2}$; $y_{\alpha3}$; $y_{\alpha4}$; $b_{\beta2}$; $b_{\beta3}$; $b_{\beta4}$ or $b_{\alpha5}$-H_2O; $y_{\beta2}$; $y_{\beta4}$-H_2O
806.434	1611.857	2	2.3	K-50 × K-128	+	α ^{048}FFKVPDNEE β ^{128}LKK	$b_{\alpha2}$; $b_{\alpha3}$; $b_{\alpha4}$; $b_{\alpha5}$; $b_{\alpha6}$; $b_{\alpha7}$; $y_{\alpha2}$-H_2O or $y_{\alpha2}$-NH_3; $y_{\alpha3}$; $y_{\alpha4}$-H_2O; $y_{\alpha5}$; $y_{\alpha6}$; $y_{\alpha7}$, $b_{\alpha7}$-NH_3, or $b_{\alpha7}$-H_2O; $b_{\beta2}$ or $b_{\alpha8}$ or $y_{\alpha8}$
810.385	1619.759	2	2.5	K-129 × K-200	+	α ^{129}KABSVEVE β ^{200}KSAmF	$b_{\alpha3}$; $b_{\alpha4}$; $b_{\alpha5}$; $b_{\alpha6}$; $b_{\alpha7}$; $y_{\alpha5}$; $y_{\alpha6}$; $b_{\beta2}$; $b_{\beta4}$ or $b_{\alpha7}$-H_2O; $y_{\beta2}$-H_2O; $y_{\beta4}$
903.934	1806.856	2	2.6	K-50 × K-200	+	α ^{048}FFKVPDNEE β ^{200}KSAMF	$b_{\alpha3}$; $b_{\alpha4}$; $b_{\alpha5}$; $b_{\alpha6}$; $b_{\alpha8}$ or $y_{\alpha8}$; $y_{\alpha2}$-H_2O; $y_{\alpha3}$; $y_{\alpha4}$; $y_{\alpha5}$ or $b_{\alpha4}$; $y_{\alpha6}$; $y_{\alpha7}$ or $b_{\alpha7}$-H_2O; $b_{\beta1}$-NH_3; $b_{\beta2}$; $b_{\beta3}$; $b_{\beta4}$, $b_{\alpha8}$-H_2O, or $y_{\alpha8}$-H_2O; $y_{\beta2}$; $y_{\beta4}$
903.932	1806.856	2	0.2	K-50 × K-200	−	α ^{048}FFKVPDNEE β ^{200}KSAMF	$b_{\alpha3}$; $b_{\alpha4}$; $b_{\alpha5}$; $b_{\alpha6}$; $b_{\alpha7}$; $b_{\alpha8}$ or $y_{\alpha8}$; $b_{\alpha8}$-H_2O, $y_{\alpha8}$-H_2O, or $b_{\beta4}$; $y_{\alpha2}$ or $b_{\beta2}$-H_2O; $y_{\alpha2}$-H_2O; $y_{\alpha3}$; $y_{\alpha5}$ or $b_{\alpha4}$; $y_{\alpha6}$; $y_{\alpha7}$ or $b_{\alpha7}$-H_2O; $y_{\alpha7}$-NH_3, $y_{\alpha7}$-H_2O, or $b_{\beta3}$-NH_3; $b_{\beta1}$-NH_3; $b_{\beta2}$; $b_{\beta3}$; $b_{\beta4}$-H_2O; $y_{\beta2}$; $y_{\beta4}$-NH_3
911.931	1822.851	2	2.3	K-50 × K-200	+	α ^{048}FFKVPDNEE β ^{200}KSAmF	$b_{\alpha3}$-NH_3; $b_{\alpha4}$; $b_{\alpha6}$-NH_3; $b_{\alpha7}$; $y_{\alpha3}$; $y_{\alpha5}$; $y_{\alpha6}$; $y_{\alpha7}$, $b_{\alpha7}$-NH_3, or $b_{\alpha7}$-H_2O; $y_{\alpha7}$-NH_3, $y_{\alpha7}$-H_2O, or $b_{\beta3}$; $y_{\alpha8}$ or $b_{\alpha8}$; $b_{\beta1}$-NH_3; $b_{\beta2}$; $b_{\beta3}$-H_2O; $b_{\beta4}$, $b_{\alpha8}$-NH_3, $b_{\alpha8}$-H_2O, $y_{\alpha8}$-NH_3, or $y_{\alpha8}$- H_2O; $y_{\beta4}$
911.929	1822.851	2	−0.2	K-50 × K-200	−	α ^{048}FFKVPDNEE β ^{200}KSAmF	$b_{\alpha3}$; $b_{\alpha4}$; $b_{\alpha6}$; $b_{\alpha7}$; $b_{\alpha8}$ or $y_{\alpha8}$; $b_{\alpha8}$-H_2O, $b_{\alpha8}$-NH_3, $y_{\alpha8}$-H_2O, $y_{\alpha8}$-NH_3, or $b_{\beta4}$; $y_{\alpha3}$; $y_{\alpha5}$; $y_{\alpha6}$; $y_{\alpha7}$-H_2O or $b_{\beta3}$; $b_{\beta1}$-NH_3; $b_{\beta2}$-NH_3; $b_{\beta3}$-H_2O; $y_{\beta2}$; $y_{\beta4}$
924.464	1847.915	2	2.6	K-50 × K-29	+	α ^{048}FFKVPDNEE β ^{027}WYKK	$b_{\alpha3}$; $b_{\alpha4}$; $b_{\alpha6}$; $b_{\alpha7}$; $b_{\alpha8}$ or $y_{\alpha8}$; $y_{\alpha3}$; $y_{\alpha5}$; $y_{\alpha6}$; $b_{\beta3}$; $y_{\beta2}$
981.983	1962.957	2	1.1	K-50 × K-200	+	α ^{048}FFKVPDNEE β ^{199}RKSAMF	$b_{\alpha3}$; $b_{\alpha4}$; $b_{\alpha6}$; $b_{\alpha7}$; $b_{\alpha8}$ or $y_{\alpha8}$; $y_{\alpha3}$; $y_{\alpha5}$; $y_{\alpha6}$; $y_{\alpha7}$ or $b_{\alpha7}$-H_2O; $y_{\alpha7}$-H_2O or $b_{\beta4}$; $b_{\beta3}$; $b_{\beta5}$, $b_{\alpha8}$-NH_3, or $b_{\alpha8}$-NH_3; $y_{\beta4}$-NH_3
988.025	1975.036	2	3.0	K-50 × K-126	+	α ^{048}FFKVPDNEE β ^{123}SIYKLK	$b_{\alpha3}$; $b_{\alpha4}$; $b_{\alpha7}$-NH_3 or $y_{\alpha7}$; $y_{\alpha4}$; $y_{\alpha5}$; $y_{\alpha6}$; $y_{\alpha7}$-NH_3; $y_{\alpha8}$, $b_{\alpha8}$, or $b_{\beta5}$; $y_{\beta4}$-NH_3
767.100	2299.281	3	2.1	K-142 × K-128	+	α ^{137}AEQQGKLLTPEEVVDR β ^{127}LKK	$b_{\alpha3}$; $b_{\alpha4}$; $b_{\alpha5}$; $b_{\alpha6}$; $b_{\alpha7}$; $b_{\alpha8}$; $b_{\alpha9}$; $b_{\alpha9}$, $y_{\alpha6}$-NH_3, or $y_{\beta2}$; $b_{\alpha11}$-H_2O; $b_{\alpha12}$; $b_{\alpha15}$; $y_{\alpha3}$; $y_{\alpha5}$-NH_3; $y_{\alpha6}$; $y_{\alpha7}$; $y_{\alpha8}$; $y_{\alpha9}$; $y_{\alpha10}$; $y_{\alpha12}$; $y_{\alpha13}$-H_2O; $y_{\alpha14}$; $b_{\beta2}$-NH_3

dx.doi.org/10.1021/bi300064v | *Biochemistry* 2012, 51, 4932−4949

Table 1. continued

m/z measured	calcd protonated molecular mass (Da)	charge state	mass deviation (ppm)	cross-linked amino acids in GCAP-2	with (+) or without (−) calcium	amino acids sequences	fragments
832.100	2494.280	3	2.2	K-142 × K-200	+	α ^{137}AEQQGKLLTPEEVVDR β ^{200}KSAMF	$b_{\alpha6}$; $b_{\alpha7}$; $b_{\alpha8}$ or $b_{\beta4}$; $b_{\alpha8}$-NH_3; $b_{\alpha9}$-NH_3 or $b_{\alpha9}$-H_2O; $b_{\alpha10}$-H_2O or $b_{\alpha10}$-NH_3; $b_{\alpha10}$-H_2O, $b_{\alpha10}$-NH_3, $y_{\alpha10}$-H_2O, or $y_{\alpha10}$-NH_3; $b_{\alpha11}$-H_2O; $b_{\alpha12}$; $b_{\alpha13}$ or $b_{\beta2}$-H_2O; $b_{\alpha13}$-NH_3; $b_{\alpha14}$; $b_{\alpha15}$; $y_{\alpha3}$; $y_{\alpha4}$; $y_{\alpha5}$-H_2O; $y_{\alpha6}$; $y_{\alpha7}$; $y_{\alpha8}$; $y_{\alpha9}$; $y_{\alpha10}$; $y_{\alpha11}$; $y_{\alpha13}$-NH_3; $y_{\alpha14}$; $y_{\alpha15}$-NH_3 or $y_{\alpha15}$-H_2O; $b_{\beta1}$; $b_{\beta2}$; $b_{\beta3}$; $y_{\beta2}$; $y_{\beta4}$
1249.593	2498.173	2	1.8	K-50 × K-200	+	α ^{048}FFKVPDNEEATQYVE β ^{200}KSAMF	$b_{\alpha3}$; $b_{\alpha4}$; $b_{\alpha5}$-H_2O; $b_{\alpha6}$; $b_{\alpha7}$; $b_{\alpha8}$; $b_{\alpha9}$; $b_{\alpha10}$; $b_{\alpha11}$; $b_{\alpha12}$; $b_{\alpha13}$; $b_{\alpha14}$ or $y_{\alpha14}$; $y_{\alpha3}$; $y_{\alpha4}$; $y_{\alpha5}$; $y_{\alpha7}$; $y_{\alpha8}$-H_2O or $y_{\alpha8}$-NH_3; $y_{\alpha10}$; $y_{\alpha11}$; $y_{\alpha12}$; $y_{\alpha13}$; $y_{\alpha13}$-H_2O or $b_{\beta3}$-NH_3; $y_{\alpha14}$-NH_3, $b_{\alpha14}$-NH_3, or $b_{\beta4}$; $y_{\beta4}$
833.396	2498.173	3	0.3	K-50 × K-200	−	α ^{048}FFKVPDNEEATQYVE β ^{200}KSAMF	$b_{\alpha4}$; $b_{\alpha9}$; $b_{\alpha10}$; $b_{\alpha11}$; $b_{\alpha12}$; $b_{\alpha12}$ or $y_{\alpha12}$; $b_{\alpha13}$; $b_{\alpha14}$ or $y_{\alpha14}$; $b_{\alpha14}$-H_2O, $y_{\alpha14}$-H_2O, or $b_{\beta4}$; $y_{\alpha2}$; $y_{\alpha3}$; $y_{\alpha6}$ or $b_{\beta2}$; $y_{\alpha11}$; $y_{\alpha12}$; $y_{\alpha13}$ or $b_{\beta2}$; $y_{\beta2}$
1249.590	2498.173	2	−0.1	K-50 × K-200	−	α ^{048}FFKVPDNEEATQYVE β ^{200}KSAMF	$b_{\alpha3}$; $b_{\alpha4}$; $b_{\alpha6}$; $b_{\alpha7}$; $b_{\alpha8}$; $b_{\alpha9}$; $b_{\alpha10}$; $b_{\alpha11}$; $b_{\alpha12}$; $b_{\alpha13}$; $b_{\alpha14}$ or $y_{\alpha14}$; $b_{\alpha14}$-H_2O, $y_{\alpha14}$-H_2O, or $b_{\beta4}$; $y_{\alpha3}$; $y_{\alpha4}$; $y_{\alpha5}$ or $y_{\alpha11}$-NH_3; $y_{\alpha5}$-H_2O; $y_{\alpha6}$; $y_{\alpha8}$; $y_{\alpha9}$; $y_{\alpha11}$; $y_{\alpha12}$; $b_{\beta3}$; $b_{\beta3}$-NH_3 or $y_{\alpha13}$-H_2O; $b_{\beta4}$-H_2O or $b_{\beta4}$-NH_3; $y_{\beta4}$
836.394	2507.159	3	2.8	K-30 × K-200	+	α ^{030}KFLEEBPSGTLFMHE β ^{200}KSAMF	$b_{\alpha2}$; $b_{\alpha3}$ or $b_{\beta2}$; $b_{\alpha4}$; $b_{\alpha5}$; $b_{\alpha6}$; $b_{\alpha9}$-H_2O; $b_{\alpha11}$; $b_{\alpha14}$; $b_{\alpha14}$-H_2O or $b_{\beta4}$; $y_{\alpha2}$; $y_{\alpha3}$; $y_{\alpha4}$; $y_{\alpha5}$; $y_{\alpha6}$; $y_{\alpha7}$-NH_3 or $y_{\alpha7}$-H_2O; $y_{\alpha8}$; $y_{\alpha9}$; $y_{\alpha9}$ or $b_{\beta1}$-NH_3; $y_{\alpha10}$; $y_{\alpha11}$; $y_{\alpha12}$; $y_{\alpha13}$; $y_{\alpha13}$, $b_{\beta4}$-NH_3, or $b_{\beta4}$-H_2O; $b_{\beta2}$-NH_3; $b_{\beta3}$; $y_{\beta2}$
1257.590	2514.168	2	1.7	K-50 × K-200	+	α ^{048}FFKVPDNEEATQYVE β ^{200}KSAmF	$b_{\alpha3}$; $b_{\alpha4}$; $b_{\alpha5}$; $b_{\alpha6}$; $b_{\alpha7}$; $b_{\alpha8}$ or $y_{\alpha7}$; $b_{\alpha9}$; $b_{\alpha10}$; $b_{\alpha11}$; $b_{\alpha12}$; $b_{\alpha13}$; $b_{\alpha14}$ or $y_{\alpha14}$; $b_{\alpha14}$-H_2O. $y_{\alpha14}$-H_2O. or $b_{\beta4}$; $y_{\alpha3}$; $y_{\alpha5}$ or $y_{\alpha11}$-NH_3; $y_{\alpha6}$; $y_{\alpha8}$-H_2O; $y_{\alpha11}$; $y_{\alpha12}$; $y_{\alpha13}$; $y_{\alpha13}$-H_2O or $b_{\beta3}$; $b_{\beta3}$-NH_3 or $b_{\beta3}$-H_2O; $b_{\beta4}$-H_2O
1257.588	2514.168	2	0.2	K-50 × K-200	−	α ^{048}FFKVPDNEEATQYVE β ^{200}KSAmF	$b_{\alpha3}$; $b_{\alpha4}$; $b_{\alpha6}$; $b_{\alpha7}$; $b_{\alpha8}$; $b_{\alpha9}$; $b_{\alpha10}$; $b_{\alpha11}$; $b_{\alpha12}$; $b_{\alpha13}$; $b_{\alpha14}$ or $y_{\alpha14}$; $b_{\alpha14}$-H_2O. $y_{\alpha14}$-H_2O. or $b_{\beta4}$; $y_{\alpha4}$; $y_{\alpha5}$ or $y_{\alpha11}$-NH_3; $y_{\alpha6}$; $y_{\alpha7}$-H_2O; $y_{\alpha9}$; $y_{\alpha10}$; $y_{\alpha11}$; $y_{\alpha12}$; $y_{\alpha13}$; $y_{\alpha13}$-H_2O or $b_{\beta3}$; $y_{\beta3}$; $y_{\beta4}$
1135.228	3403.661	3	2.8	K-178 × K-200	+	α ^{177}DKWVMKMLQMDLNPSSWISQQR β ^{200}KSAMF	$b_{\alpha2}$; $b_{\alpha6}$; $b_{\alpha9}$; $b_{\alpha10}$; $b_{\alpha11}$; $b_{\alpha12}$; $b_{\alpha13}$; $b_{\alpha15}$; $b_{\alpha16}$; $b_{\alpha17}$; $b_{\alpha18}$; $b_{\alpha19}$; $b_{\alpha20}$; $b_{\alpha21}$; $y_{\alpha4}$; $y_{\alpha5}$; $y_{\alpha6}$; $y_{\alpha7}$; $y_{\alpha8}$ or $b_{\alpha19}$; $y_{\alpha9}$; $y_{\alpha9}$ or $y_{\alpha18}$-NH_3; $y_{\alpha10}$; $y_{\alpha10}$ or $y_{\alpha15}$; $y_{\alpha12}$; $y_{\alpha13}$; $y_{\alpha17}$ or $b_{\beta3}$-NH_3; $b_{\beta3}$-NH_3; $b_{\beta4}$

[a]Abbreviations: B, carbamidomethylated Cys; m, oxidized Met.

dx.doi.org/10.1021/bi300064v | *Biochemistry* 2012, 51, 4932−4949

Table 2. Intermolecular Cross-Links between GCAP-2 and GC Peptide, Cross-Linked with BS^2G[a]

m/z measured	calcd protonated molecular mass (Da)	charge state	mass deviation (ppm)	cross-linked amino acid in GCAP-2	with (+) or without (−) calcium	amino acid sequences	fragments
510.759	1020.512	2	−0.5	K-200	−	α ^{200}KSAMF β ^{001}YR	$b_{\alpha1}$-NH_3 or $b_{\alpha1}$-H_2O; $b_{\alpha2}$; $b_{\alpha3}$; $b_{\alpha4}$; $b_{\beta1}$-H_2O; $y_{\alpha1}$; $y_{\alpha2}$; $y_{\beta1}$
518.757	1036.507	2	−0.4	K-200	+	α ^{200}KSAmF β ^{001}YR	$b_{\alpha2}$; $b_{\alpha3}$; $b_{\alpha4}$; $b_{\beta1}$-H_2O; $y_{\alpha1}$; $y_{\alpha2}$; $y_{\alpha3}$; $y_{\alpha4}$
531.291	1061.572	2	3.3	K-29	+	α ^{027}WYKK β ^{001}YR	$b_{\alpha2}$; $b_{\alpha3}$; $b_{\beta1}$; $y_{\alpha2}$; $y_{\alpha3}$; $y_{\beta1}$
588.812	1176.613	2	2.5	K-200	+	α ^{199}RKSAMF β ^{001}YR	$b_{\alpha2}$; $b_{\alpha4}$; $b_{\alpha5}$; $b_{\beta1}$; $y_{\alpha5}$; $y_{\beta1}$
594.850	1188.692	2	0.0	K-126	−	α ^{123}SIYKLK β ^{001}YR	$b_{\alpha2}$; $b_{\alpha4}$; $b_{\alpha5}$; $b_{\beta1}$; $y_{\alpha2}$; $y_{\alpha3}$; $y_{\alpha4}$; $y_{\beta1}$
594.851	1188.692	2	2.8	K-126	+	α ^{123}SIYKLK β ^{001}YR	$b_{\alpha4}$; $b_{\alpha5}$; $b_{\beta1}$; $y_{\alpha3}$; $y_{\alpha4}$; $y_{\beta1}$
622.327	1243.644	2	2.6	K-178	+	α ^{177}DKWVMK β ^{001}YR	$b_{\alpha2}$; $b_{\alpha3}$; $b_{\alpha4}$; $b_{\alpha5}$; $y_{\alpha2}$; $y_{\alpha5}$
623.822	1246.636	2	−0.0	K-106	−	α ^{103}IYDKDR β ^{001}YR	$b_{\alpha5}$ or $b_{\beta1}$; $y_{\alpha1}$ or $y_{\beta1}$; $y_{\alpha2}$; $y_{\alpha3}$; $y_{\alpha4}$
630.358	1259.708	2	0.1	K-98	−	α ^{097}LKWTFK β ^{001}YR	$b_{\alpha2}$; $b_{\alpha3}$; $b_{\alpha4}$; $b_{\alpha5}$; $b_{\beta1}$; $y_{\alpha2}$; $y_{\alpha3}$; $y_{\alpha4}$
630.360	1259.708	2	3.1	K-98	+	α ^{097}LKWTFK β ^{001}YR	$b_{\alpha3}$; $b_{\alpha4}$; $b_{\alpha5}$; $b_{\beta1}$; $y_{\alpha2}$; $y_{\alpha3}$; $y_{\alpha4}$
679.832	1358.656	2	0.3	K-129	−	α ^{129}KABSVEVE β ^{001}YR	$b_{\alpha2}$; $b_{\alpha3}$; $b_{\alpha4}$; $b_{\alpha5}$; $b_{\alpha6}$; $b_{\alpha7}$; $y_{\alpha2}$; $y_{\alpha3}$; $y_{\alpha6}$
679.832	1358.656	2	0.7	K-129	+	α ^{129}KABSVEVE β ^{001}YR	$b_{\alpha2}$; $b_{\alpha3}$; $b_{\alpha5}$; $b_{\alpha6}$; $b_{\alpha7}$; $y_{\alpha2}$
467.255	1399.745	3	3.3	K-178	+	α ^{176}RDKWVMK β ^{001}YR	$b_{\alpha1}$ or $y_{\beta1}$-H_2O; $b_{\alpha2}$; $b_{\alpha4}$; $b_{\alpha5}$; $b_{\alpha6}$; $b_{\beta1}$ or; $y_{\alpha6}$-H_2O; $y_{\alpha1}$; $y_{\alpha2}$; $y_{\alpha4}$; $y_{\alpha5}$; $y_{\alpha6}$
781.378	1561.747	2	0.4	K-50	−	α ^{048}FFKVPDNEE β ^{001}YR	$b_{\alpha3}$; $b_{\alpha4}$; $b_{\alpha5}$; $b_{\alpha6}$;$b_{\alpha7}$; $y_{\alpha3}$; $y_{\alpha5}$; $y_{\alpha6}$; $y_{\alpha7}$
781.380	1561.747	2	3.1	K-50	+	α ^{048}FFKVPDNEE β ^{001}YR	$b_{\alpha2}$; $b_{\alpha3}$; $b_{\alpha6}$; $b_{\alpha7}$; $b_{\beta1}$; $y_{\alpha3}$; $y_{\alpha5}$; $y_{\alpha6}$; $y_{\alpha7}$
603.649	1808.927	3	3.3	K-102	+	α ^{099}WTFKIYDKDR β ^{001}YR	$b_{\alpha4}$; $b_{\alpha7}$; $y_{\alpha1}$; $y_{\alpha2}$; $y_{\alpha3}$ or $b_{\alpha4}$-NH_3; $b_{\alpha9}$ or $b_{\beta1}$; $y_{\alpha4}$; $y_{\alpha5}$; $y_{\alpha8}$; $b_{\alpha7}$
711.991	2133.956	3	0.6	S-37	−	α ^{031}FLEEBPSGTLFMHE β ^{001}YR	$b_{\alpha2}$; $b_{\alpha3}$; $b_{\alpha6}$; $b_{\alpha9}$; $b_{\alpha13}$ or $y_{\alpha13}$; $y_{\alpha2}$; $y_{\alpha4}$; $y_{\alpha5}$; $y_{\alpha9}$; $y_{\alpha10}$; $y_{\alpha11}$; $y_{\alpha12}$
1125.090	2249.171	2	0.2	K-142	−	α ^{137}AEQQGKLLTPEEVVDR β ^{001}YR	$b_{\alpha7}$; $b_{\alpha8}$; $b_{\alpha9}$; $b_{\alpha10}$; $b_{\alpha11}$; $b_{\alpha12}$; $b_{\alpha14}$; $y_{\alpha4}$; $y_{\alpha5}$; $y_{\alpha7}$; $y_{\alpha8}$; $y_{\alpha10}$; $y_{\alpha12}$; $y_{\alpha14}$
1125.092	2249.171	2	2.9	K-142	+	α ^{137}AEQQGKLLTPEEVVDR β ^{001}YR	$b_{\alpha6}$; $b_{\alpha7}$; $b_{\alpha8}$; $b_{\alpha9}$; $b_{\alpha11}$; $b_{\alpha13}$; $b_{\alpha14}$; $y_{\alpha4}$; $y_{\alpha5}$; $y_{\alpha8}$; $y_{\alpha11}$; $y_{\alpha14}$; $y_{\alpha15}$-H_2O
750.396	2249.171	3	0.5	K-142	−	α ^{137}AEQQGKLLTPEEVVDR β ^{001}YR	$b_{\alpha7}$; $b_{\alpha8}$; $b_{\alpha9}$; $y_{\alpha7}$; $y_{\alpha8}$; $y_{\alpha9}$; $y_{\alpha10}$; $y_{\alpha12}$
750.398	2249.171	3	3.3	K-142	+	α ^{137}AEQQGKLLTPEEVVDR β ^{001}YR	$b_{\alpha3}$; $b_{\alpha7}$; $b_{\alpha8}$; $b_{\alpha9}$; $y_{\alpha7}$; $y_{\alpha8}$; $y_{\alpha9}$; $y_{\alpha10}$; $y_{\alpha11}$; $y_{\alpha12}$; $y_{\alpha13}$; $y_{\alpha14}$
1127.037	2253.065	2	0.5	K-50	−	α ^{048}FFKVPDNEEATQYVE β ^{001}YR	$b_{\alpha3}$; $b_{\alpha4}$; $b_{\alpha8}$; $b_{\alpha9}$; $b_{\alpha10}$; $b_{\alpha11}$; $b_{\alpha12}$; $b_{\alpha13}$; $b_{\alpha14}$ or $y_{\alpha14}$; $y_{\alpha3}$; $y_{\alpha11}$; $y_{\alpha12}$
754.689	2262.051	3	0.9	K-30	−	α ^{030}KFLEEBPSGTLFMHE β ^{001}YR	$b_{\alpha4}$; $b_{\alpha5}$; $b_{\alpha6}$; $b_{\alpha8}$; $b_{\alpha11}$; $y_{\alpha4}$; $y_{\alpha5}$; $y_{\alpha9}$; $y_{\alpha10}$; $y_{\alpha11}$

[a]Abbreviation: B, carbamidomethylated Cys; m, oxidized Met.

products within GCAP-2 as well as intermolecular cross-linked products between GCAP-2 and GC peptide (Tables 1 and 2). Five cross-linked products indicate an identical interaction site between GCAP-2 and GC peptide as in the mixture with calcium, except for Lys-29, Lys-102, Lys-178, and Lys-200, which were not found to be cross-linked. Lys-30, Ser-37, and Lys-106 were exclusively found in the calcium-free sample. These cross-links did not allow differentiation between GCAP-2−GC peptide interaction in the absence and presence of calcium, apart from a stronger cross-linking involvement of the N-terminal GCAP-2 part in the presence of calcium. Thus, we conducted further experiments with two GC peptides, in which the photoreactive amino acid photo-Leu was incorporated at position 5 or 13 of the GC peptide (Scheme 1).

Identification of Sites of Contact between GCAP-2 and GC Peptides by Photoaffinity Labeling. To get a closer look at the structure of the GCAP-2−GC peptide complex and to delineate differences of the interaction in the absence and presence of calcium, we employed two modified GC peptides. In each of these peptides, one amino acid was exchanged with photo-Leu

dx.doi.org/10.1021/bi300064v | *Biochemistry* 2012, 51, 4932−4949

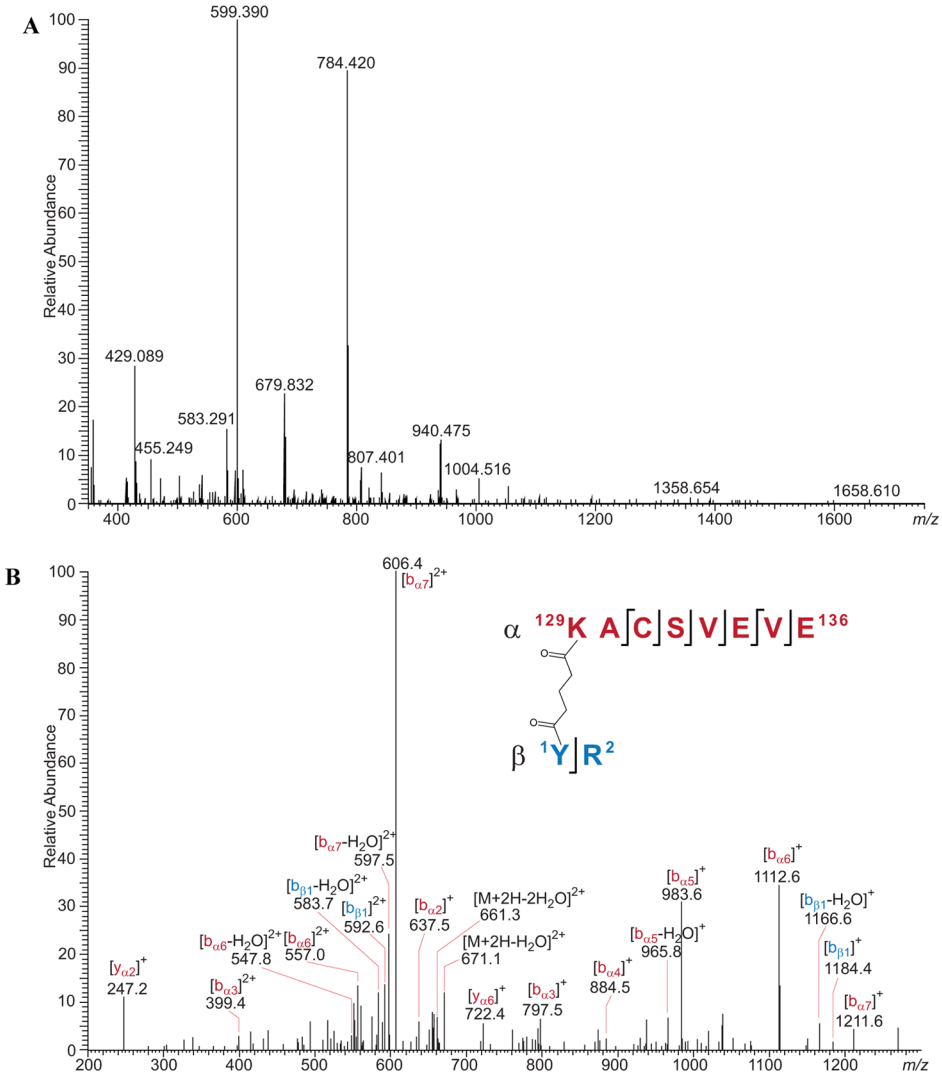

Figure 2. Identification of a BS^2G cross-link between Lys-129 of GCAP-2 and Tyr-1 of GC peptide in the presence of calcium (100-fold molar excess of BS^2G, 60 min reaction). (A) Mass spectrum recorded at 51.8 min. The signal at m/z 679.832 was selected for MS/MS. (B) Fragment ion mass spectrum of the precursor ion at m/z 679.832. GCAP-2 peptide (amino acids 129−136, carbamidomethylated Cys-131) fragment ions are colored red; GC peptide (amino acids 1 and 2) fragment ions are colored blue.

bearing a diazirine moiety. In GC photopeptide 1, Val-5 was replaced with photo-Leu, whereas in GC photopeptide 2, Leu-13 was exchanged (Scheme 1). Using both peptides in a complementary fashion, we sought to obtain a more detailed model for the GCAP-2−GC peptide complex as two different hinge points are present for the photo-cross-linking reaction in the GC peptides. Moreover, as the photo-Leu side chain is short compared to BS^2G, it was expected to yield information about directly interacting amino acids. SDS−PAGE of the cross-linking reaction mixture of GCAP-2 with photo-Leu GC peptides in the absence of calcium showed weak signals for the GCAP-2−GC peptide complex (1:1).

Several cross-linked products (two for GC photopeptide 1 and four for GC photopeptide 2) were identified in calcium-loaded GCAP-2−GC peptide complexes, which conclusively point to five distinct interaction sites (Figure 3 and Tables 3 and 4). In the calcium-loaded state, photo-Leu-5 of GC photopeptide 1 was found to have reacted with either Val-61, Glu-62, or Ala-63, located within the α-helix at the beginning of the second EF-hand motif, and with A-57 or T-58 in the same EF-hand motif. Because of the poor quality of the spectra, the latter two amino acids were excluded as a basis for structural modeling. Val-61 was considered to be the most likely cross-linking site on the basis of the obtained MS/MS data (Table 3). GC photopeptide 2 was found to have reacted with Phe-204 in the C-terminal region of GCAP-2, with amino acids Phe-170−Glu-172 in the second α-helix of EF-hand motif 4, and with amino acids Pro-146 and Glu-147 at the beginning of EF-hand motif 4. Because these sites are clearly separated in the 3D structure of calcium-loaded GCAP-2, a significant conformational shift must have occurred to accommodate these cross-links. As the 14 C-terminal amino acids of GCAP-2 (amino acids Ser-191−Phe-204) are not resolved in the NMR structure (PDB entry 1JBA), it is not possible to draw any conclusions about the structure of the C-terminus, but our cross-linking results provide hints about its high flexibility.

In the calcium-free state, a signal of a doubly charged ion at m/z 844.453 appeared in the ESI mass spectra pointing to a cross-link between the photo-Leu at position 13 of GC peptide 2 and Ala-137 or Glu-138 of GCAP-2 (Figure 4), located in a

dx.doi.org/10.1021/bi300064v | Biochemistry 2012, 51, 4932−4949

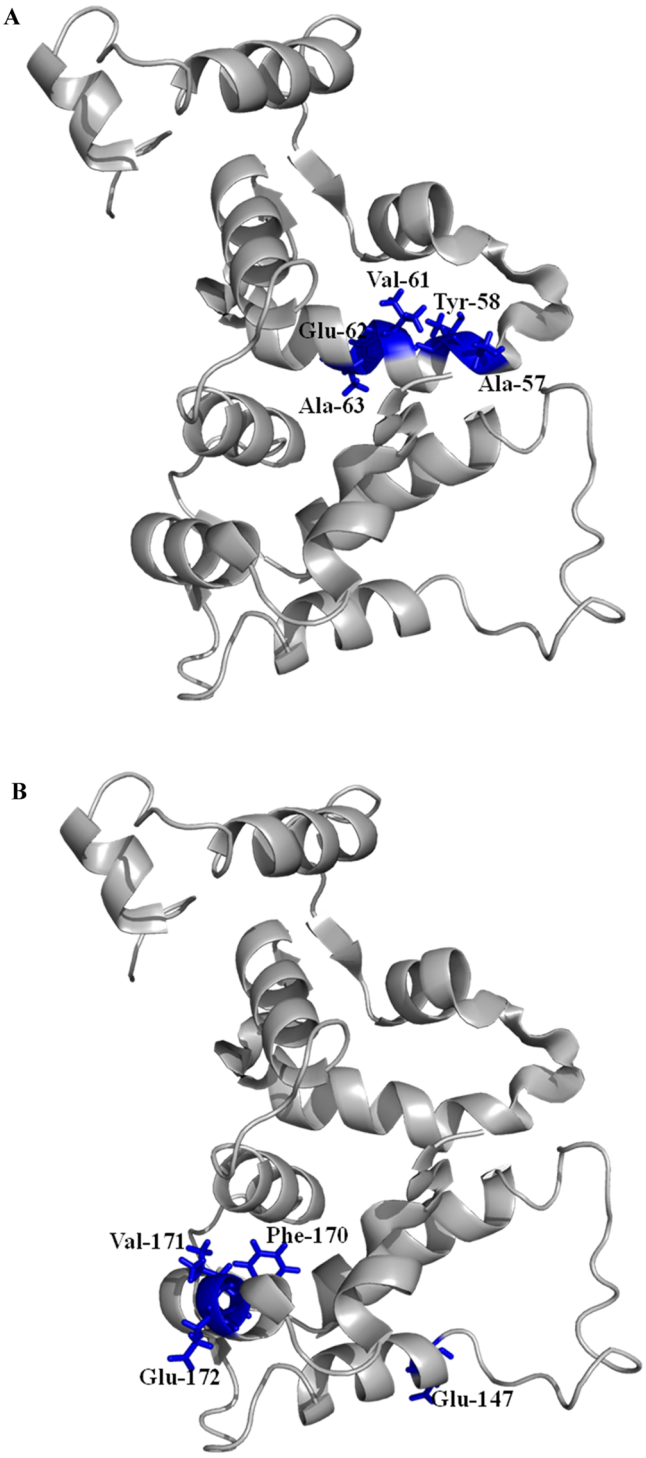

Figure 3. NMR structure of nonmyristoylated GCAP-2 in the calcium-loaded state (PDB entry 1JBA). Cross-linked amino acids after reaction with (A) GC photopeptide 1 and (B) GC photopeptide 2 are shown as blue sticks.

loop region between EF-hand motifs 3 and 4. Additionally, we identified a number of cross-links from several widely dispersed parts of GCAP-2 for both GC photopeptides. As no specific binding site emerged, we assume a high flexibility of GCAP-2 accompanied by a major structural change within GCAP-2 upon peptide binding in the absence of calcium.

Creating a Model for the GCAP-2−GC Peptide Complex. The half-helical structure predicted by PSIPRED (data not shown) was experimentally confirmed by CD spectroscopy. In aqueous solution, no secondary structure was observed. Upon addition of TFE, typical α-helical signals (maximum at ∼190 nm and two minima at ∼208 and ∼220 nm) emerged, indicating that the peptide engages a partly helical structure (Figure S4, Supporting Information) and supporting the PSIPRED prediction. During the first 10 ns of the production run, distance constraints between calcium-loaded GCAP-2 and the GC peptide determined from chemical cross-linking and photoaffinity labeling were applied to selected amino acids and enforced via a stepwise increased biasing force (Table S3, Supporting Information). All amino acid pairs were affected by the biasing force except the Tyr-1/Lys-126 and Tyr-1/Lys-129 pairs. This indicates a less favored state, although it fulfills nearly all constraints determined by the cross-linking experiments. For a consecutive period of 20 ns (data not shown for the last 10 ns), we removed the restraints to obtain a relaxed, nonbiased structure, which should approximate the native conformation of the GCAP-2−GC peptide complex. After the initially applied biasing force had been removed, the distances among the cross-linked amino acids Glu-147, Phe-170, and Val-171 reached an average value beyond the maximal distance defined for the photoreactive amino acid (9 Å). Keeping the fluctuation in mind, we can neglect this violation. No constraint violations (for the average distance) could be observed for the amino acids cross-linked with BS^2G (Table S4, Supporting Information).

In Figure 5, one can see that after 20 ns the GC peptide exhibits a mainly α-helical conformation. We would like to point out that the structure proposed herein is intended to give first insights into the potential mode of binding of ROS-GC 1 to GCAP-2. As such, this stucture will serve as basis for creating more refined structures of the ROS-GC 1−GCAP-2 complex.

DISCUSSION

A combination of chemical cross-linking and photoaffinity labeling experiments followed by an in-depth mass spectrometric analysis of the created cross-linked products allowed us to gain valuable insights into the structure of the complex between myristoylated GCAP-2 and peptides derived from the postulated binding site in the catalytic region of ROS-GC 1. Our experiments confirmed this postulated GCAP-2 binding site as GCAP-2−GC peptide (1:1) complexes were obtained after the cross-linking reactions. In the absence of calcium, the structure of GCAP-2 appeared to be much more flexible than that in the presence of calcium, as indicated by the large number of both intra- and intermolecular cross-links in the absence of calcium. On the other hand, only a limited number of cross-links were obtained in the presence of calcium, pointing to a structurally well-defined complex between GCAP-2 and the GC peptide. The intramolecular cross-links of N-terminally myristoylated GCAP-2 were in agreement with the published NMR structure of nonmyristoylated GCAP-2, indicating that the myristoylation does not induce a conformational change in GCAP-2. We found a number of cross-links with the C-terminal region of GCAP-2 indicating a high degree of flexibility in the C-terminus of GCAP-2. Interestingly, the 14 C-terminal amino acids are not present in the NMR structure, presumably because of the high flexibility of the C-terminal region. As such, our cross-linking data are in agreement with the available structural GCAP-2 data.

dx.doi.org/10.1021/bi300064v | *Biochemistry* 2012, 51, 4932−4949

Table 3. Intermolecular Cross-Links between Peptides of GCAP-2 and GC Photopeptide 1 (photo-Leu-5)[a]

m/z measured	calcd protonated molecular mass (Da)	charge state	mass deviation (ppm)	amino acids of GCAP-2 cross-linked with GC peptide	with (+) or without (−) calcium	amino acid sequences	fragments
545.777	1090.546	2	−0.3	F-204	−	α ^{201}SAMF β ^{003}IHUNR	$b_{\alpha3}$-H_2O or $y_{\beta2}$-NH_3; $y_{\alpha1}$; $y_{\alpha2}$; $y_{\alpha3}$; $b_{\beta2}$; $y_{\beta2}$; $y_{\beta3}$; $y_{\beta4}$; β
432.565	1295.682	3	−0.3	A-137, E-138	−	α ^{137}AEQQGK β ^{003}IHUNR	$b_{\alpha5}$; $y_{\alpha1}$; $y_{\alpha2}$; $y_{\alpha4}$; $b_{\beta2}$; $y_{\beta2}$; $y_{\beta3}$; $y_{\beta4}$; α; β
648.344	1295.682	2	−0.1	A-137, E-138	−	α ^{137}AEQQGK β ^{003}IHUNR	$b_{\alpha2}$; $b_{\alpha3}$; $b_{\alpha4}$; $b_{\alpha5}$; $y_{\alpha2}$; $y_{\alpha3}$; $y_{\alpha4}$; $y_{\alpha5}$; $b_{\beta2}$; $b_{\beta4}$; $y_{\beta2}$; $y_{\beta3}$; $y_{\beta4}$; α; β
438.574	1313.707	3	−0.4	F-170, V-171 alternative A-174	−	α ^{170}FVEGAR β ^{003}IHUNR	$b_{\alpha3}$; $b_{\alpha4}$; $y_{\alpha1}$ or $y_{\beta1}$; $y_{\alpha3}$; $y_{\alpha4}$; $y_{\alpha5}$; $b_{\beta2}$; $y_{\beta2}$; $y_{\beta3}$; $y_{\beta4}$; α; β $y_{\alpha4}$
440.577	1319.718	3	−0.7	G-91, T-92, L-93 alternative E-94−K-96, L-93−K-96	−	α ^{091}GTLEHK β ^{003}IHUNR	$b_{\alpha3}$; $b_{\alpha4}$; $b_{\alpha5}$; $y_{\alpha1}$; $y_{\alpha4}$ or $y_{\beta3}$; $b_{\beta2}$; $b_{\beta4}$; $y_{\beta3}$; $y_{\beta4}$; β $b_{\alpha3}$ (alternative E-94−K-96); $y_{\alpha4}$ (alternative L-93−K-96)
668.883	1336.758	2	0.3	I-120 alternative V-121, E-122, L117−D119	−	α ^{117}LLDIVE β ^{003}IHUNR	$b_{\alpha3}$; $b_{\alpha4}$ or $y_{\alpha4}$-H_2O; $b_{\alpha5}$; $y_{\alpha2}$; $y_{\alpha3}$-H_2O; $y_{\alpha4}$; $y_{\alpha5}$ or $y_{\beta4}$; $b_{\beta2}$; $b_{\beta3}$; $b_{\beta4}$; $y_{\beta2}$; $y_{\beta3}$; α; β $y_{\alpha2}$-H_2O (alternative V-121−E-122); $b_{\alpha3}$ (alternative L-117−D-119)
714.849	1428.690	2	0.1	V-133, E-134 alternative E-134−E-136	−	α ^{130}ABSVEVE β ^{003}IHUNR	$b_{\alpha5}$; $b_{\alpha6}$; $y_{\alpha5}$; $b_{\beta2}$; $b_{\beta3}$; $b_{\beta4}$; $y_{\beta2}$; $y_{\beta3}$; $y_{\beta4}$; α; β $y_{\alpha3}$ (alternative E-134−E-136)
482.260	1444.766	3	−0.5	Y-104	−	α ^{103}IYDKDR β ^{003}IHUNR	$b_{\alpha3}$; $b_{\alpha5}$; $y_{\alpha1}$ or $y_{\beta1}$; $y_{\alpha3}$; $y_{\alpha4}$; $y_{\alpha5}$ or $y_{\beta4}$; $b_{\beta2}$; $y_{\beta2}$; $y_{\beta3}$
742.417	1483.827	2	0.3	V-157, D-158	−	α ^{153}IFLLVDE β ^{003}IHUNR	$b_{\alpha2}$; $b_{\alpha3}$; $b_{\alpha4}$; $b_{\alpha6}$; $y_{\alpha3}$; $y_{\alpha4}$; $y_{\alpha5}$; $y_{\alpha6}$; $b_{\beta2}$; $b_{\beta3}$; $b_{\beta4}$; $y_{\beta2}$; $y_{\beta3}$; β
587.296	1759.876	3	−0.9	V-51	−	α ^{048}FFKVPDNEE β ^{003}IHUNR	$b_{\alpha2}$; $b_{\alpha3}$; $b_{\alpha4}$; $b_{\alpha5}$-NH_3; $b_{\alpha8}$ or $y_{\alpha8}$; $y_{\alpha4}$; $y_{\alpha4}$-NH_3, $y_{\alpha7}$, $b_{\alpha7}$-NH_3, or $b_{\alpha7}$-H_2O; $y_{\alpha6}$; $y_{\alpha7}$; $b_{\beta2}$; $b_{\beta4}$-NH_3 or $b_{\beta4}$-H_2O; $y_{\beta3}$; $y_{\beta4}$; α; β
602.667	1805.987	3	−0.3	E-148, V-149	−	α ^{143}LLTPEEVVDR β ^{003}IHUNR	$b_{\alpha2}$; $b_{\alpha3}$; $b_{\alpha7}$; $b_{\alpha9}$ or $b_{\beta4}$; $y_{\alpha1}$ or $y_{\beta1}$; $y_{\alpha6}$-NH_3; $y_{\alpha7}$; $y_{\alpha8}$; $y_{\beta2}$; $y_{\beta3}$
617.649	1850.933	3	−0.5	A-63	−	α ^{057}ATQYVEAMFR β ^{003}IHUNR	$b_{\alpha3}$; $y_{\alpha1}$ or $y_{\beta1}$; $y_{\alpha3}$; $y_{\alpha4}$; $y_{\alpha5}$; $y_{\alpha6}$; $y_{\alpha7}$; $y_{\alpha8}$; $b_{\beta2}$; $y_{\beta3}$; $y_{\beta4}$; α; β
617.649	1850.933	3	−0.4	V-61 alternative E-62, A-63	+	α ^{057}ATQYVEAMFR β ^{003}IHUNR	$b_{\alpha4}$; $b_{\alpha5}$; $b_{\alpha6}$; $b_{\alpha7}$; $y_{\alpha3}$; $y_{\beta4}$; $y_{\alpha5}$-NH_3 or β; $y_{\alpha6}$; $y_{\alpha7}$; $y_{\alpha8}$; $y_{\alpha9}$; $b_{\beta2}$; $y_{\beta3}$; $y_{\beta4}$; α $y_{\alpha5}$ (alternative E-62−A-63)
622.981	1866.928	3	−0.3	E-62−R-66	−	α ^{057}ATQYVEAmFR β ^{003}IHUNR	$y_{\alpha5}$; $y_{\beta6}$; $y_{\alpha7}$; $y_{\alpha8}$; $y_{\alpha9}$; $b_{\beta2}$; $b_{\beta3}$; $y_{\beta2}$; $y_{\beta3}$; $y_{\beta4}$; α; β
638.346	1913.024	3	−0.6	Q-115−D-119	−	α ^{115}QELLDIVE β ^{003}YRIHUNR	$b_{\alpha5}$; $b_{\alpha6}$; $b_{\alpha7}$; $y_{\alpha2}$; $b_{\beta6}$; $y_{\beta6}$ or $b_{\alpha7}$-NH_3
676.993	2028.962	3	0.7	T-58, Q-59	−	α ^{051}VPDNEEATQYVE β ^{003}IHUNR	$b_{\alpha9}$; $b_{\alpha10}$; $b_{\alpha11}$ or $y_{\alpha5}$-H_2O; $y_{\alpha5}$-NH_3; $y_{\alpha7}$-NH_3; $y_{\alpha9}$; $y_{\alpha10}$; $y_{\alpha11}$; $b_{\beta2}$; $b_{\beta3}$; $b_{\beta4}$; $y_{\beta2}$; $y_{\beta3}$; $y_{\alpha4}$-H_2O
676.992	2028.962	3	0.2	A-57, T-58	+	α ^{051}VPDNEEATQYVE β ^{003}IHUNR	$b_{\alpha4}$; $b_{\alpha9}$; $b_{\alpha10}$; $b_{\alpha11}$ or $y_{\alpha5}$-H_2O; $y_{\alpha4}$; $y_{\alpha6}$-NH_3; $y_{\alpha10}$; $y_{\alpha11}$; $b_{\beta4}$
690.673	2070.003	3	0.4	A-137−Q-140	−	α ^{130}ABSVEVEAEQQGK β ^{003}IHUNR	$b_{\alpha2}$; $b_{\alpha3}$ or β; $b_{\alpha11}$; $y_{\alpha6}$; $y_{\alpha7}$; $y_{\alpha8}$; $y_{\alpha9}$; $y_{\alpha10}$; $y_{\alpha11}$; $y_{\beta3}$; α
760.372	2279.101	3	0.2	A-10−V-16	−	α ^{010}AEENGAVGAADAAQLQE β ^{003}IHUNR	$b_{\alpha7}$; $b_{\alpha11}$; $b_{\alpha12}$; $b_{\alpha13}$; $b_{\beta14}$; $b_{\alpha15}$; $b_{\beta16}$; $y_{\alpha2}$; $y_{\alpha3}$; $y_{\alpha5}$ or $b_{\alpha13}$

[a]Abbreviations: U, photo-Leu; B, carbamidomethylated Cys; m, oxidized Met.

Also, in the presence of calcium, only a small number of well-defined intermolecular photo-cross-links between GCAP-2 and GC peptides (two with GC photopeptide 1 and four with GC photopeptide 2) were obtained. This limited number of cross-links between GCAP-2 and photo-GC peptides indicates a well-defined orientation of the GC peptide in the complex with GCAP-2 in the presence of calcium. In the absence of calcium, on the other hand, we found a larger number of intermolecular photo-cross-links (16 with GC photopeptide 1 and 16 with GC photopeptide 2), suggesting a less well-defined structure between GCAP-2 and GC peptide.

Our data provide the first insights into the structure of GCAP-2−GC peptide complexes, for which only limited information is available. Future cross-linking experiments will target GC domains to gain a more detailed molecular knowledge of the mechanisms underlying formation of the complex between GCAP-2 and ROS-GC 1. We are also planning to introduce mutations at specific amino acids that have been found to be essential for GCAP-2−GC peptide interaction. The final goal is to establish a structural model for the GCAP-2−full-length ROS-GC 1 complex, which will be essential for developing novel drugs targeting this system.

dx.doi.org/10.1021/bi300064v | *Biochemistry* 2012, 51, 4932−4949

Table 4. Intermolecular Cross-Links between Peptides of GCAP-2 and GC Photopeptide 2 (photo-Leu-13)[a]

m/z measured	calcd protonated molecular mass (Da)	charge state	mass deviation (ppm)	amino acids of GCAP-2 cross-linked with GC peptide	with (+) or without (−) calcium	amino acid sequences	fragments
645.357	1289.706	2	0.5	D-177, K-178	−	α ^{177}DK β ^{008}STVQIUSALN	$b_{\beta3}$; $b_{\beta4}$; $b_{\beta5}$; $b_{\beta6}$; $b_{\beta7}$; $b_{\beta8}$; $b_{\beta9}$; $y_{\beta2}$; $y_{\beta4}$; $y_{\beta5}$; $y_{\beta6}$; $y_{\beta7}$; $y_{\beta8}$; α; $b_{\beta8}$-NH_3 or β
741.885	1482.762	2	0.1	F-204	−	α ^{201}SAMF β ^{008}STVQIUSALN	$b_{\alpha3}$; $y_{\alpha1}$; $y_{\alpha2}$; $b_{\beta3}$-H_2O; $b_{\beta4}$; $b_{\beta5}$; $b_{\beta6}$; $b_{\beta7}$; $b_{\beta8}$; $b_{\beta9}$; $y_{\beta2}$; $y_{\beta4}$; $y_{\beta5}$; $y_{\beta6}$; α; β
741.885	1482.762	2	0.4	F-204	+	α ^{201}SAMF β ^{008}STVQIUSALN	$b_{\alpha3}$; $y_{\alpha1}$; $y_{\alpha2}$; $b_{\beta3}$; $b_{\beta4}$; $b_{\beta5}$; $b_{\beta6}$; $b_{\beta7}$; $b_{\beta8}$; $b_{\beta9}$; $y_{\beta2}$; $y_{\beta4}$; $y_{\beta5}$; $y_{\beta6}$; α; β
749.882	1498.757	2	0	F-204	+	α ^{201}SAmF β ^{008}STVQIUSALN	$b_{\alpha3}$; $y_{\alpha1}$; $y_{\alpha2}$; $b_{\beta5}$; $b_{\beta6}$; $b_{\beta7}$; $b_{\beta8}$; $b_{\beta9}$; $y_{\beta4}$; $y_{\beta5}$; $y_{\beta6}$; $y_{\beta7}$; α; β
768.391	1535.773	2	0.6	V-133	−	α ^{130}ACSVE β ^{008}STVQIUSALN	$b_{\alpha4}$; $y_{\alpha2}$ or $b_{\beta8}$-H_2O; $y_{\alpha2}$-NH_3; $b_{\beta4}$; $b_{\beta5}$; $b_{\beta6}$; $b_{\beta7}$; $b_{\beta8}$; $b_{\beta9}$; $y_{\beta2}$; $y_{\beta4}$; $y_{\beta5}$; $y_{\beta6}$; $y_{\beta7}$
769.433	1537.858	2	−0.1	Y-125	−	α ^{123}SIYK β ^{008}STVQIUSALN	$b_{\alpha3}$; $y_{\alpha2}$; $y_{\alpha3}$; $b_{\beta3}$; $b_{\beta4}$; $b_{\beta5}$; $b_{\beta6}$; $b_{\beta7}$; $b_{\beta8}$; $y_{\beta2}$-NH_3; $y_{\beta4}$; $y_{\beta5}$; $y_{\beta6}$; $y_{\beta7}$; $y_{\beta8}$; α
844.453	1687.897	2	0.5	A-137, E-138	−	α ^{137}AEQQGK β ^{008}STVQIUSALN	$b_{\alpha2}$; $b_{\alpha3}$; $b_{\alpha4}$; $b_{\alpha5}$; $y_{\alpha3}$; $y_{\alpha4}$; $b_{\beta3}$-H_2O; $b_{\beta4}$; $b_{\beta5}$; $b_{\beta6}$; $b_{\beta7}$; $b_{\beta8}$; $b_{\beta9}$; $y_{\beta4}$; $y_{\beta5}$; $y_{\beta6}$; $y_{\beta7}$; $y_{\beta8}$; α; β
568.961	1704.870	3	−0.6	C-111, I-112	−	α ^{109}NGCIDR β ^{008}STVQIUSALN alternative N-109−C-111	$b_{\alpha5}$, $y_{\alpha4}$, or $b_{\beta5}$-H_2O; $y_{\alpha1}$; $y_{\alpha2}$; $y_{\alpha5}$-H_2O or $y_{\alpha5}$-NH_3; $b_{\beta2}$; $b_{\beta3}$; $b_{\beta5}$; $b_{\beta6}$; $b_{\beta7}$; $b_{\beta8}$; $b_{\beta9}$ or $y_{\alpha5}$-NH_3; $y_{\beta2}$; $y_{\beta4}$; $y_{\beta5}$; $y_{\beta6}$; $y_{\beta7}$; $y_{\beta8}$, $y_{\alpha4}$-H_2O, or $y_{\alpha4}$-NH_3; β $b_{\alpha3}$ (alternative N-109−C-111)
852.939	1704.870	2	0.5	G-110−I-112 alternative N-109−C-111	−	α ^{109}NGCIDR β ^{008}STVQIUSALN	$b_{\alpha4}$; $b_{\alpha5}$; $y_{\alpha2}$; $y_{\alpha5}$; $b_{\beta3}$-H_2O; $b_{\beta4}$; $b_{\beta5}$; $b_{\beta6}$; $b_{\beta8}$; $b_{\beta9}$ or $y_{\alpha5}$-NH_3; $y_{\beta4}$; $y_{\beta5}$; $y_{\beta6}$; $y_{\beta7}$; $y_{\beta8}$, $y_{\alpha4}$-H_2O, or $y_{\alpha4}$-NH_3 $b_{\alpha3}$ (alternative N-109−C-111)
569.312	1705.923	3	−0.7	V-171, E-172	−	α ^{170}FVEGAR β ^{008}STVQIUSALN	$b_{\alpha3}$-NH_3; $b_{\alpha4}$ or $b_{\beta8}$; $y_{\alpha1}$; $y_{\alpha3}$; $y_{\alpha4}$; $y_{\alpha5}$-NH_3 or β; $b_{\beta2}$; $b_{\beta3}$-H_2O; $b_{\beta6}$; $b_{\beta7}$; $b_{\beta9}$; $y_{\beta2}$-NH_3 or $y_{\alpha2}$-H_2O; $y_{\beta4}$; $y_{\beta5}$; $y_{\beta6}$; $y_{\beta7}$; $y_{\beta8}$; $y_{\beta9}$; α; β
853.465	1705.923	2	0	V-171, E-172	−	α ^{170}FVEGAR β ^{008}STVQIUSALN	$b_{\alpha3}$; $b_{\alpha4}$; $b_{\alpha5}$; $y_{\alpha3}$; $y_{\alpha5}$-NH_3 or $y_{\alpha5}$-H_2O; $b_{\beta3}$; $b_{\beta4}$; $b_{\beta5}$; $b_{\beta6}$; $b_{\beta7}$; $b_{\beta8}$; $b_{\beta9}$; $y_{\beta3}$; $y_{\beta4}$; $y_{\beta5}$; $y_{\beta6}$; $y_{\beta7}$; $y_{\beta9}$; α; β
853.466	1705.923	2	0.5	F-170−E-172	+	α ^{170}FVEGAR β ^{008}STVQIUSALN	$b_{\alpha3}$; $b_{\alpha5}$; $y_{\alpha2}$; $y_{\alpha3}$; $b_{\beta3}$-H_2O; $b_{\beta4}$; $b_{\beta5}$; $b_{\beta6}$; $b_{\beta8}$; $b_{\beta9}$; $y_{\beta4}$; $y_{\beta5}$; $y_{\beta6}$; $y_{\beta7}$; α; β
569.312	1705.923	3	−0.3	F-170	+	α ^{170}FVEGAR β ^{008}STVQIUSALN	$y_{\alpha1}$; $y_{\alpha2}$; $y_{\alpha3}$; $y_{\alpha4}$; $y_{\alpha5}$-NH_3 or β; $b_{\beta2}$; $b_{\beta3}$-H_2O; $b_{\beta4}$; $b_{\beta6}$; $b_{\beta7}$-NH_3 or $b_{\beta7}$-H_2O; $b_{\beta8}$; $b_{\beta9}$; $y_{\beta4}$; $y_{\beta5}$; $y_{\beta6}$; $y_{\beta7}$; $y_{\beta8}$; α; β+H_2O
571.316	1711.934	3	−1.0	L-93	−	α ^{091}GTLEHK β ^{008}STVQIUSALN	$b_{\alpha3}$-H_2O or $y_{\beta6}$-NH_3; $b_{\alpha5}$, $b_{\beta9}$-H_2O, or $b_{\beta9}$-NH_3; $y_{\alpha4}$-H_2O or $b_{\beta5}$-NH_3; $b_{\beta2}$; $b_{\beta3}$; $b_{\beta6}$; $b_{\beta8}$; $b_{\beta9}$; $y_{\beta2}$; $y_{\beta5}$; $y_{\beta6}$; $y_{\beta7}$; $y_{\beta8}$; $y_{\beta9}$-NH_3
856.471	1711.934	2	0.3	L-93, E-94	−	α ^{091}GTLEHK β ^{008}STVQIUSALN	$b_{\alpha4}$-NH_3; $b_{\alpha5}$; $y_{\alpha2}$; $y_{\alpha4}$; $b_{\beta3}$; $b_{\beta4}$; $b_{\beta5}$; $b_{\beta6}$; $b_{\beta7}$; $b_{\beta8}$; $b_{\beta9}$; $y_{\beta5}$; $y_{\beta6}$-NH_3; $y_{\beta7}$; $y_{\beta8}$; α; β
865.434	1729.860	2	0.5	V-51	−	α ^{051}VPDNEE β ^{008}STVQIUSALN	$b_{\alpha3}$; $b_{\alpha5}$; $y_{\alpha5}$; $b_{\beta3}$-H_2O; $b_{\beta4}$; $b_{\beta5}$; $b_{\beta6}$; $b_{\beta7}$; $b_{\beta8}$; $b_{\beta9}$; $y_{\beta4}$; $y_{\beta5}$; $y_{\beta6}$; $y_{\beta7}$; $y_{\beta8}$; α; β
869.455	1737.902	2	0.2	T-58	−	α ^{057}ATQYVE β ^{008}STVQIUSALN	$b_{\alpha2}$; $b_{\alpha3}$; $b_{\alpha4}$; $b_{\alpha5}$-NH_3; $y_{\alpha2}$; $y_{\alpha3}$-H_2O; $y_{\alpha5}$; $b_{\beta5}$; $b_{\beta6}$; $b_{\beta7}$-NH_3 or $b_{\beta7}$-H_2O; $b_{\beta8}$-H_2O; $b_{\beta9}$; $y_{\beta3}$; $y_{\beta4}$; $y_{\beta5}$; $y_{\beta6}$; $y_{\beta7}$-NH_3or $y_{\beta7}$-H_2O; $y_{\beta8}$; $y_{\beta9}$; α
882.446	1763.884	2	0.6	V-133 alternative E-134, V-135; A-130, C-131	−	α ^{130}ACSVEVE β ^{008}STVQIUSALN	$b_{\alpha4}$; $b_{\alpha5}$; $b_{\alpha6}$; $y_{\alpha2}$; $y_{\alpha3}$; $y_{\alpha4}$-NH_3; $y_{\alpha5}$; $b_{\beta3}$; $b_{\beta5}$; $b_{\beta6}$; $b_{\beta7}$; $b_{\beta8}$; $b_{\beta9}$; $y_{\beta3}$; $y_{\beta4}$; $y_{\beta5}$; $y_{\beta6}$; $y_{\beta7}$-NH_3; $y_{\beta8}$; $y_{\beta9}$-NH_3; α $y_{\alpha3}$-NH_3 (alternative E-134, V-135); $b_{\alpha2}$ or $y_{\alpha5}$ (alternative A-130, C-131)
631.331	1891.979	3	−0.6	K-129−C-131 alternative A-130, C-131	−	α ^{129}KACSVEVE β ^{008}STVQIUSALN	$b_{\alpha3}$; $b_{\alpha5}$; $b_{\alpha6}$; $b_{\alpha7}$; $y_{\alpha2}$; $y_{\alpha3}$; $b_{\beta3}$; $b_{\beta4}$-H_2O; $b_{\beta5}$ or $y_{\beta7}$-H_2O; $b_{\beta7}$; $b_{\beta8}$-H_2O, $b_{\alpha6}$-NH_3, or $b_{\alpha6}$-H_2O; $b_{\beta9}$; $y_{\beta2}$; $y_{\beta4}$; $y_{\beta5}$; $y_{\beta6}$; $y_{\beta7}$; $y_{\beta8}$; α or $b_{\alpha7}$-NH_3 $y_{\alpha7}$-H_2O (alternative A-130, C-131)

dx.doi.org/10.1021/bi300064v | Biochemistry 2012, 51, 4932−4949

Table 4. continued

m/z measured	calcd protonated molecular mass (Da)	charge state	mass deviation (ppm)	amino acids of GCAP-2 cross-linked with GC peptide	with (+) or without (−) calcium	amino acid sequences	fragments
946.494	1891.979	2	0.0	K-129−C-131	−	α ^{129}KACSVEVE β ^{008}STVQIUSALN	$b_{\alpha3}$; $b_{\alpha4}$; $b_{\alpha5}$; $b_{\alpha6}$; $b_{\alpha7}$; $y_{\alpha3}$; $y_{\alpha5}$; $b_{\beta3}$; $b_{\beta5}$; $b_{\beta6}$; $b_{\beta7}$-NH_3; $b_{\beta8}$; $b_{\beta9}$; $y_{\beta3}$; $y_{\beta4}$; $y_{\beta5}$; $y_{\beta6}$; $y_{\beta7}$; $y_{\beta8}$-NH_3; α or $b_{\alpha7}$-NH_3 or $b_{\alpha7}$-H_2O
				alternative C-131			$y_{\alpha6}$; $y_{\alpha7}$-H_2O (alternative C-131)
639.341	1916.008	3	0.7	A-137	−	α ^{135}VEAEQQGK β ^{008}STVQIUSALN	$b_{\alpha3}$-H_2O; $b_{\alpha6}$, $y_{\beta8}$-NH_3, or $y_{\alpha5}$-H_2O; $b_{\alpha6}$-NH_3 or $b_{\alpha6}$-H_2O; $b_{\alpha7}$-H_2O; $y_{\alpha2}$; $y_{\alpha3}$; $y_{\alpha4}$; $y_{\alpha5}$, $b_{\beta9}$-NH_3, or $b_{\beta9}$-H_2O; $y_{\alpha6}$; $y_{\alpha7}$; $b_{\beta3}$; $b_{\beta6}$; $b_{\beta7}$; $b_{\beta8}$ or $y_{\alpha6}$-NH_3; $b_{\beta8}$-NH_3 or $b_{\beta8}$-H_2O; $b_{\beta9}$; $y_{\beta2}$; $y_{\beta4}$-NH_3; $y_{\beta5}$; $y_{\beta6}$; $y_{\beta7}$; $y_{\beta8}$; $y_{\beta9}$; α; β-NH_3
				alternative V135, E-136			$b_{\alpha2}$ (alternative V135, E-136)
654.661	1961.971	3	−1.3	N-109, G-110	−	α ^{109}NGCIDRQE β ^{008}STVQIUSALN	$b_{\alpha2}$ or $b_{\alpha7}$-NH_3; $b_{\alpha3}$-NH_3 or $b_{\alpha3}$-H_2O; $b_{\alpha4}$ or $y_{\beta5}$-H_2O; $b_{\alpha5}$ or $y_{\beta6}$-NH_3; $b_{\alpha5}$-H_2O; $b_{\alpha7}$ or $b_{\beta9}$-NH_3; $b_{\alpha7}$-NH_3 or $b_{\alpha7}$-H_2O; $y_{\alpha2}$-H_2O; $y_{\alpha3}$; $y_{\alpha4}$; $y_{\alpha6}$; $y_{\alpha7}$-NH_3 or $b_{\beta9}$; $b_{\beta3}$-H_2O; $b_{\beta5}$ or $y_{\alpha4}$-H_2O; $b_{\beta6}$; $b_{\beta8}$; $y_{\beta2}$-NH_3; $y_{\beta4}$; $y_{\beta5}$; $y_{\beta6}$; $y_{\beta7}$; $y_{\beta8}$; $y_{\beta9}$; β
981.490	1961.971	2	0.6	N-109, G-110	−	α ^{109}NGCIDRQE β ^{008}STVQIUSALN	$b_{\alpha2}$-H_2O; $b_{\alpha3}$; $b_{\alpha4}$ or $y_{\beta5}$-H_2O; $b_{\alpha4}$-NH_3; $b_{\alpha5}$; $b_{\alpha6}$; $b_{\alpha7}$; $y_{\alpha3}$; $y_{\alpha4}$; $y_{\alpha5}$; $y_{\alpha6}$; $y_{\alpha7}$; $b_{\beta4}$-H_2O; $b_{\beta6}$; $b_{\beta7}$; $b_{\beta8}$; $b_{\beta9}$, $y_{\alpha7}$-NH_3, or $y_{\alpha7}$-H_2O; $y_{\beta3}$-NH_3; $y_{\beta4}$; $y_{\beta5}$; $y_{\beta6}$; $y_{\beta8}$; $y_{\beta9}$
673.669	2018.992	3	−0.4	N-109, G-110	−	α ^{109}NGBIDRQE β ^{008}STVQIUSALN	$b_{\alpha2}$-NH_3 or $b_{\beta8}$; $b_{\alpha4}$ or $y_{\beta5}$-NH_3; $b_{\alpha5}$-H_2O; $b_{\alpha6}$-NH_3; $b_{\alpha7}$, $b_{\beta9}$-NH_3, or $b_{\beta9}$-H_2O; $b_{\alpha7}$-H_2O; $y_{\alpha2}$; $y_{\alpha3}$; $y_{\alpha5}$-NH_3 or $y_{\alpha5}$-H_2O; $y_{\alpha7}$-NH_3 or $b_{\beta9}$; $b_{\beta5}$-NH_3; $b_{\beta6}$; $b_{\beta7}$; $b_{\beta8}$; $y_{\beta2}$; $y_{\beta4}$; $y_{\beta5}$; $y_{\beta6}$; $y_{\beta7}$; $y_{\beta8}$; $y_{\beta9}$; α; β-NH_3
733.406	2198.203	3	−0.6	E-147	+	α ^{143}LLTPEEVVDR β ^{008}STVQIUSALN	$b_{\alpha2}$ or $y_{\beta2}$-H_2O; $b_{\alpha3}$; $y_{\alpha3}$; $y_{\alpha4}$; $y_{\alpha5}$; $y_{\alpha6}$-H_2O; $y_{\alpha7}$; $y_{\alpha8}$; $y_{\alpha9}$-NH_3, $y_{\alpha9}$-H_2O, or $b_{\beta9}$; $b_{\beta6}$; $b_{\beta8}$, $y_{\alpha8}$-H_2O, or $y_{\alpha8}$-NH_3; $b_{\beta9}$-NH_3 or $b_{\beta9}$- H_2O; $y_{\beta5}$; $y_{\beta6}$; $y_{\beta7}$; $y_{\beta8}$; $y_{\beta9}$; α; β
1211.094	2421.178	2	1.0	V-51	−	α ^{051}VPDNEEATQYVE β ^{008}STVQIUSALN	$b_{\alpha1}$-NH_3; $b_{\alpha3}$-NH_3 or $b_{\alpha3}$-H_2O; $b_{\alpha6}$; $b_{\alpha7}$; $b_{\alpha8}$; $b_{\alpha9}$; $b_{\alpha10}$ or $b_{\beta8}$; $b_{\alpha11}$-NH_3; $y_{\alpha3}$; $y_{\alpha4}$; $y_{\alpha5}$; $y_{\alpha7}$; $y_{\alpha8}$; $b_{\beta7}$; ($b_{\beta8}$); $b_{\beta9}$; $y_{\beta4}$; $y_{\beta5}$; $y_{\beta6}$; α; β
				alternative E-55, E-56, E-62			$y_{\alpha8}$ (alternative E-55); $b_{\alpha5}$ or $y_{\alpha7}$ (alternative E-56); $b_{\alpha5}$, $b_{\alpha9}$, $b_{\alpha10}$-H_2O, or $b_{\alpha11}$ (alternative E-62)

[a]Abbreviations: U, photo-Leu; B, carbamidomethylated Cys; m, oxidized Met.

dx.doi.org/10.1021/bi300064v | *Biochemistry* 2012, 51, 4932−4949

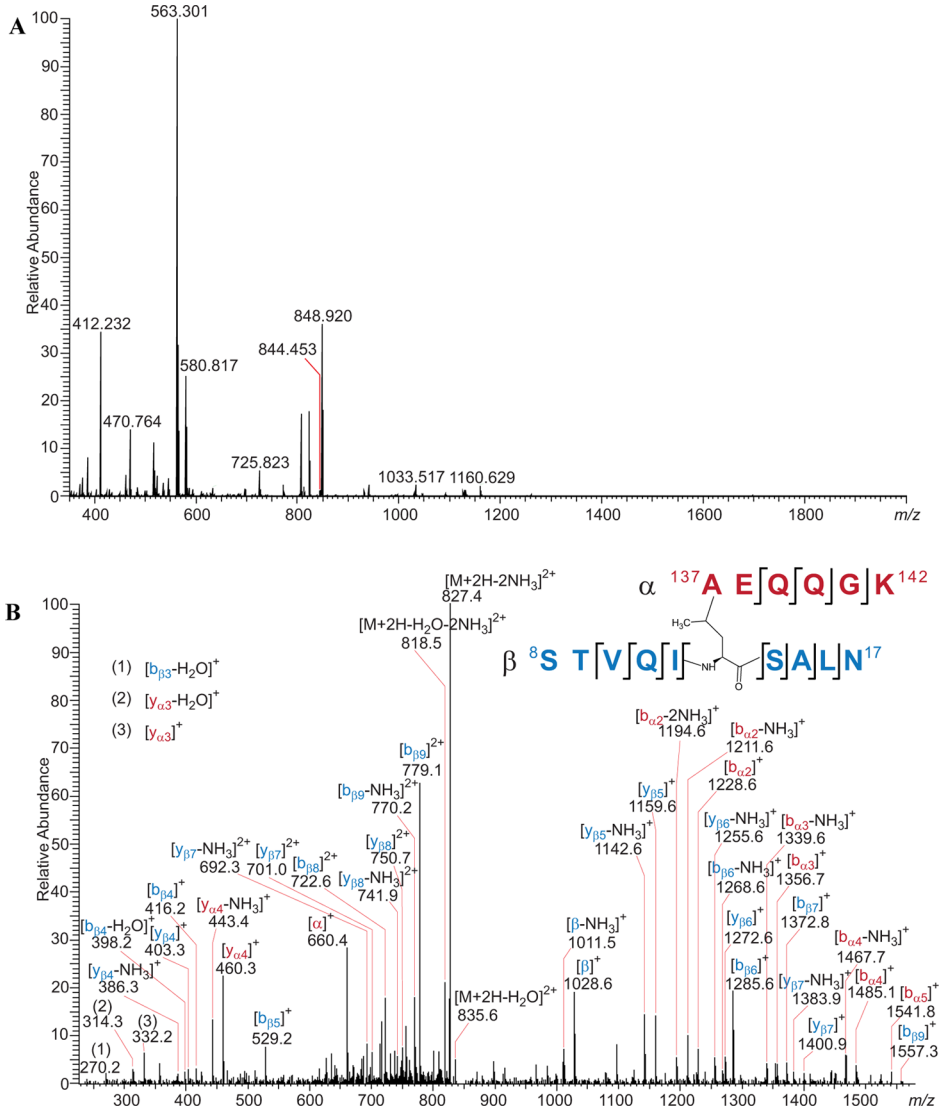

Figure 4. Identification of a photo-cross-link between Ala-137 or Glu-138 of GCAP-2 and photo-Leu-13 of GC photopeptide 2 in the absence of calcium (irradiation energy of 4000 mJ/cm^2). (A) Mass spectrum recorded at 39.8 min. The signal at m/z 844.453 was selected for MS/MS. (B) Fragment ion mass spectrum of the precursor ion at m/z 844.453. GCAP-2 peptide (amino acids 137−142) fragment ions are colored red; GC photopeptide 2 (amino acids 8−17) fragment ions are colored blue.

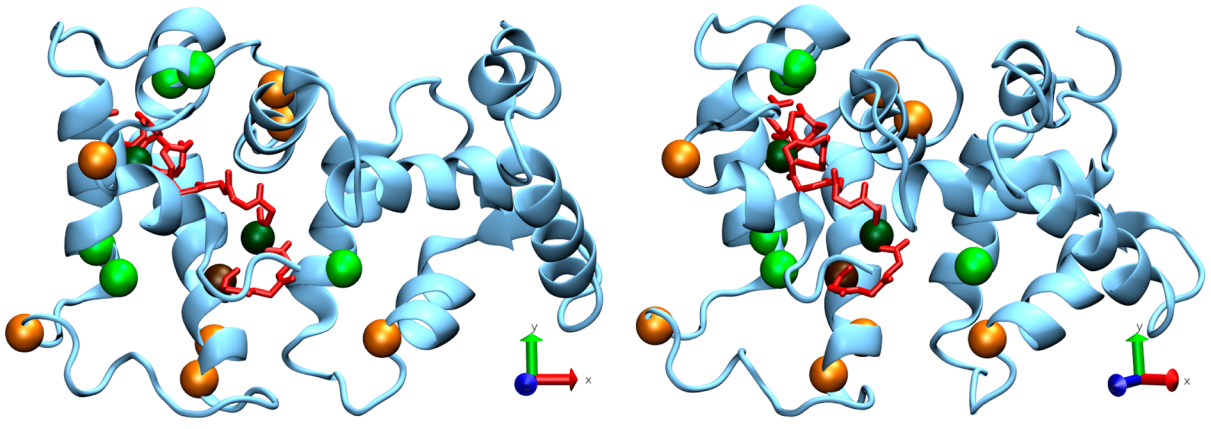

Figure 5. Structural model of the GCAP-2−GC peptide complex. The backbone of the most representative GC peptide is colored red along with GCAP-2, which is shown as a light blue cartoon. Cross-linking sites in GCAP-2 obtained from photoaffinity labeling, which were used for modeling, are shown as light green spheres. Cross-linking sites obtained with BS^{2}G, which were used for modeling, are shown as light orange spheres. The reactive sites in the GC peptide are shown as dark green (photo-Leu at positions 5 and 13) and brown (Tyr-1) spheres. The image was prepared using VMD[63] and rendered with POV-Ray (http://www.povray.org/).

dx.doi.org/10.1021/bi300064v | *Biochemistry* 2012, 51, 4932−4949

CONCLUSIONS

We showed that complementary cross-linking strategies using amine-reactive cross-linkers and photoaffinity labeling combined with high-resolution mass spectrometry yield valuable information about the molecular mechanisms underlying the interaction between myristoylated GCAP-2 and a peptide derived from the catalytic domain of ROS-GC 1. Our results indicate that myristoylation of GCAP-2 does not change the protein's overall 3D structure. The detected cross-links reveal the high flexibility of the C-terminal region of GCAP-2 as well as the high flexibility of calcium-free GCAP-2 in the complex with the GC peptide. On the basis of the distance constraints imposed by the cross-links, we were able to create a model of the complex between myristoylated GCAP-2 and the GC peptide that is formed in the presence of calcium.

ASSOCIATED CONTENT

Supporting Information

SDS−PAGE analysis of cross-linking reaction mixutres, MALDI-TOF mass spectra of intact cross-linked complexes, a visualization of intramolecular cross-linked products in GCAP-2, CD spectroscopic measurements of the GC peptide, MS data of GCAP-2 peptides that are modified with partially hydrolyzed cross-linker BS^2G, distance constraints based on cross-linking experiments, and distances that were observed in the MD simulation. This material is available free of charge via the Internet at http://pubs.acs.org.

AUTHOR INFORMATION

Corresponding Author

*Department of Pharmaceutical Chemistry and Bioanalytics, Institute of Pharmacy, Martin-Luther University Halle-Wittenberg, Wolfgang-Langenbeck-Straße 4, D-06120 Halle (Saale), Germany. Telephone: +49-345-5525170. Fax: +49-345-5527026. E-mail: andrea.sinz@pharmazie.uni-halle.de.

Funding

This work was funded by the Deutsche Forschungsgemeinschaft (DFG), Project Si 867/13-1, the BMBF ProNet-T3 (Project To-06), and the region of Sachsen-Anhalt.

Notes

The authors declare no competing financial interest.

ACKNOWLEDGMENTS

B.E.S.O. thanks Ms. Stephanie Hirst for giving support on Rosetta. Prof. Jens Meiler is acknowledged for giving critical comments about the modeling part of the manuscript.

ABBREVIATIONS

ACN, acetonitrile; BS^2G, bis(sulfosuccinimidyl)glutarate; CD, circular dichroism; CID, collision-induced dissociation; DMSO, dimethyl sulfoxide; DTT, dithiothreitol; EGTA, ethylene glycol tetraacetic acid; ESI, electrospray ionization; FA, formic acid; GCAP, guanylylcyclase-activating protein; HEPES, 4-(2-hydroxyethyl)-1-piperazineethanesulfonic acid; HPLC, high-performance liquid chromatography; IAA, iodoacetamide; LTQ, linear ion trap; MALDI-TOF, matrix-assisted laser desorption ionization time-of-flight; MS, mass spectrometry; MS/MS, tandem mass spectrometry; MD, molecular dynamics; NCS, neuronal calcium sensor; NHS, *N*-hydroxysuccinimide; PDB, Protein Data Bank; ROS-GC, rod outer segment guanylylcyclase; SDS−PAGE, sodium dodecyl sulfate−polyacrylamide gel electrophoresis; S/N, signal-to-noise; TFA, trifluoroacetic acid; TFE, trifluoroethanol.

REFERENCES

(1) Koch, K. W. (1991) Purification and Identification of Photoreceptor Guanylate-Cyclase. *J. Biol. Chem. 266*, 8634−8637.
(2) Shyjan, A. W., Desauvage, F. J., Gillett, N. A., Goeddel, D. V., and Lowe, D. G. (1992) Molecular Cloning of a Retina-Specific Membrane Guanylyl Cyclase. *Neuron 9*, 727−737.
(3) Lowe, D. G., Dizhoor, A. M., Liu, K., Gu, Q. M., Spencer, M., Laura, R., Lu, L., and Hurley, J. B. (1995) Cloning and Expression of a Second Photoreceptor-Specific Membrane Retina Guanylyl Cyclase (RetGC), RetGC-2. *Proc. Natl. Acad. Sci. U.S.A. 92*, 5535−5539.
(4) Yang, R. B., Foster, D. C., Garbers, D. L., and Fulle, H. J. (1995) Two Membrane Forms of Guanylyl Cyclase Found in the Eye. *Proc. Natl. Acad. Sci. U.S.A. 92*, 602−606.
(5) Koch, K. W., Duda, T., and Sharma, R. K. (2002) Photoreceptor specific guanylate cyclases in vertebrate phototransduction. *Mol. Cell. Biochem. 230*, 97−106.
(6) Sharma, R. K. (2010) Membrane guanylate cyclase is a beautiful signal transduction machine: Overview. *Mol. Cell. Biochem. 334*, 3−36.
(7) Dizhoor, A. M., and Hurley, J. B. (1999) Regulation of photoreceptor membrane guanylyl cyclases by guanylyl cyclase activator proteins. *Methods 19*, 521−531.
(8) Haeseleer, F., Imanishi, Y., Sokal, I., Filipek, S., and Palczewski, K. (2002) Calcium-binding proteins: Intracellular sensors from the calmodulin superfamily. *Biochem. Biophys. Res. Commun. 290*, 615−623.
(9) Peshenko, I. V., and Dizhoor, A. M. (2004) Guanylyl cyclase-activating proteins (GCAPs) are Calcium/Mg^{2+} sensors: Implications for photoreceptor guanylyl cyclase (RetGC) regulation in mammalian photoreceptors. *J. Biol. Chem. 279*, 16903−16906.
(10) Lim, S., Peshenko, I., Dizhoor, A., and Ames, J. B. (2009) Effects of Calcium, Mg^{2+}, and Myristoylation on Guanylyl Cyclase Activating Protein 1 Structure and Stability. *Biochemistry 48*, 850−862.
(11) Olshevskaya, E. V., Hughes, R. E., Hurley, J. B., and Dizhoor, A. M. (1997) Calcium binding, but not a calcium-myristoyl switch, controls the ability of guanylyl cyclase-activating protein GCAP-2 to regulate photoreceptor guanylyl cyclase. *J. Biol. Chem. 272*, 14327−14333.
(12) Hughes, R. E., Brzovic, P. S., Dizhoor, A. M., Klevit, R. E., and Hurley, J. B. (1998) Calcium-dependent conformational changes in bovine GCAP-2. *Protein Sci. 7*, 2675−2680.
(13) Stephen, R., Bereta, G., Golczak, M., Palczewski, K., and Sousa, M. C. (2007) Stabilizing function for myristoyl group revealed by the crystal structure of a neuronal calcium sensor, guanylate cyclase-activating protein 1. *Structure 15*, 1392−1402.
(14) Schröder, T., Lilie, H., and Lange, C. (2011) The myristoylation of guanylate cyclase-activating protein-2 causes an increase in thermodynamic stability in the presence but not in the absence of calcium. *Protein Sci. 20*, 1155−1165.
(15) Dizhoor, A. M., Olshevskaya, E. V., Henzel, W. J., Wong, S. C., Stults, J. T., Ankoudinova, I., and Hurley, J. B. (1995) Cloning, Sequencing, and Expression of a 24-kDa Calcium-binding Protein Activating Photoreceptor Guanylyl Cyclase. *J. Biol. Chem. 270*, 25200−25206.
(16) Gorczyca, W. A., Graykeller, M. P., Detwiler, P. B., and Palczewski, K. (1994) Purification and Physiological Evaluation of a Guanylate-Cyclase Activating Protein from Retinal Rods. *Proc. Natl. Acad. Sci. U.S.A. 91*, 4014−4018.
(17) Palczewski, K., Subbaraya, I., Gorczyca, W. A., Helekar, B. S., Ruiz, C. C., Ohguro, H., Huang, J., Zhao, X. Y., Crabb, J. W., Johnson, R. S., Walsh, K. A., Graykeller, M. P., Detwiler, P. B., and Baehr, W. (1994) Molecular Cloning and Characterization of Retinal Photoreceptor Guanylyl Cyclase-Activating Protein. *Neuron 13*, 395−404.
(18) Frins, S., Bonigk, W., Muller, F., Kellner, R., and Koch, K. W. (1996) Functional characterization of a guanylyl cyclase-activating protein from vertebrate rods: Cloning, heterologous expression, and localization. *J. Biol. Chem. 271*, 8022−8027.
(19) Haeseleer, F., Sokal, I., Li, N., Pettenati, M., Rao, N., Bronson, D., Wechter, R., Baehr, W., and Palczewski, K. (1999) Molecular characterization of a third member of the guanylyl cyclase-activating protein subfamily. *J. Biol. Chem. 274*, 6526−6535.

(20) Laura, R. P., Dizhoor, A. M., and Hurley, J. B. (1996) The membrane guanylyl cyclase, retinal guanylyl cyclase-1, is activated through its intracellular domain. *J. Biol. Chem. 271*, 11646−11651.
(21) Koch, K. W., and Stryer, L. (1988) Highly Cooperative Feedback Control of Retinal Rod Guanylate-Cyclase by Calcium Ions. *Nature 334*, 64−66.
(22) Pugh, E. N., and Lamb, T. D. (1990) Cyclic GMP and Calicium: The Internal Messengers of Excitation and Adaptation in Vertebrate Photoreceptors. *Vision Res. 30*, 1923−1948.
(23) Graykeller, M. P., and Detwiler, P. B. (1994) The Calcium Feedback Signal in the Phototransduction Cascade of Vertebrate Rods. *Neuron 13*, 849−861.
(24) Fain, G. L., Matthews, H. R., Cornwall, M. C., and Koutalos, Y. (2001) Adaptation in vertebrate photoreceptors. *Physiol. Rev. 81*, 117−151.
(25) Mendez, A., Burns, M. E., Sokal, I., Dizhoor, A. M., Baehr, W., and Chen, J. (2001) Role of guanylate cyclase-activating proteins (GCAPs) in setting the flash sensitivity of rod photoreceptors. *Proc. Natl. Acad. Sci. U.S.A. 98*, 9948−9953.
(26) Ames, J. B., Dizhoor, A. M., Ikura, M., Palczewski, K., and Stryer, L. (1999) Three-dimensional structure of guanylyl cyclase activating protein-2, a calcium-sensitive modulator of photoreceptor guanylyl cyclases. *J. Biol. Chem. 274*, 19329−19337.
(27) Wilson, E. M., and Chinkers, M. (1995) Identification of Sequences Mediating Guanylyl Cyclase Dimerization. *Biochemistry 34*, 4696−4701.
(28) Yang, R. B., and Garbers, D. L. (1997) Two eye guanylyl cyclases are expressed in the same photoreceptor cells and form homomers in preference to heteromers. *J. Biol. Chem. 272*, 13738−13742.
(29) Olshevskaya, E. V., Ermilov, A. N., and Dizhoor, A. M. (1999) Dimerization of guanylyl cyclase-activating protein and a mechanism of photoreceptor guanylyl cyclase activation. *J. Biol. Chem. 274*, 25583−25587.
(30) Lange, C., Duda, T., Beyermann, M., Sharma, R. K., and Koch, K. W. (1999) Regions in vertebrate photoreceptor guanylyl cyclase ROS-GC1 involved in calcium-dependent regulation by guanylyl cyclase-activating protein GCAP-1. *FEBS Lett. 460*, 27−31.
(31) Krylov, D. M., and Hurley, J. B. (2001) Identification of proximate regions in a complex of retinal guanylyl cyclase 1 and guanylyl cyclase-activating protein-1 by a novel mass spectrometry-based method. *J. Biol. Chem. 276*, 30648−30654.
(32) Sokal, I., Haeseleer, F., Arendt, A., Adman, E. T., Hargrave, P. A., and Palczewski, K. (1999) Identification of a guanylyl cyclase-activating protein-binding site within the catalytic domain of retinal guanylyl cyclase1. *Biochemistry 38*, 1387−1393.
(33) Duda, T., Fik-Rymarkiewicz, E., Venkataraman, V., Krishnan, R., Koch, K. W., and Sharma, R. K. (2005) The calcium-sensor guanylate cyclase activating protein type 2 specific site in rod outer segment membrane guanylate cyclase type 1. *Biochemistry 44*, 7336−7345.
(34) Dizhoor, A. M., Boikov, S. G., and Olshevskaya, E. V. (1998) Constitutive activation of photoreceptor guanylate cyclase by Y99C mutant of GCAP-1: Possible role in causing human autosomal dominant cone degeneration. *J. Biol. Chem. 273*, 17311−17314.
(35) Sokal, I., Li, N., Surgucheva, I., Warren, M. J., Payne, A. M., Bhattacharya, S. S., Baehr, W., and Palczewski, K. (1998) GCAP1-(Y99C) mutant is constitutively active in autosomal dominant cone dystrophy. *Mol. Cell 2*, 129−133.
(36) Sato, M., Nakazawa, M., Usui, T., Tanimoto, N., Abe, H., and Ohguro, H. (2005) Mutations in the gene coding for guanylate cyclase-activating protein 2 (GUCA1B gene) in patients with autosomal dominant retinal dystrophies. *Graefe's Arch. Clin. Exp. Ophthalmol. 243*, 235−242.
(37) Young, M. M., Tang, N., Hempel, J. C., Oshiro, C. M., Taylor, E. W., Kuntz, I. D., Gibson, B. W., and Dollinger, G. (2000) High throughput protein fold identification by using experimental constraints derived from intramolecular cross-links and mass spectrometry. *Proc. Natl. Acad. Sci. U.S.A. 97*, 5802−5806.
(38) Back, J. W., de Jong, L., Muijsers, A. O., and de Koster, C. G. (2003) Chemical cross-linking and mass spectrometry for protein structural modeling. *J. Mol. Biol. 331*, 303−313.
(39) Fabris, D., and Yu, E. T. (2010) Elucidating the higher-order structure of biopolymers by structural probing and mass spectrometry: MS3D. *J. Mass Spectrom. 45*, 841−860.
(40) Sinz, A. (2006) Chemical cross-linking and mass spectrometry to map three-dimensional protein structures and protein-protein interactions. *Mass Spectrom. Rev. 25*, 663−682.
(41) Sinz, A. (2010) Investigation of protein-protein interactions in living cells by chemical crosslinking and mass spectrometry. *Anal. Bioanal. Chem. 397*, 3433−3440.
(42) Lee, Y. J. (2008) Mass spectrometric analysis of cross-linking sites for the structure of proteins and protein complexes. *Mol. BioSyst. 4*, 816−823.
(43) Zhang, H. Z., Tang, X. T., Munske, G. R., Tolic, N., Anderson, G. A., and Bruce, J. E. (2009) Identification of Protein-Protein Interactions and Topologies in Living Cells with Chemical Cross-linking and Mass Spectrometry. *Mol. Cell. Proteomics 8*, 409−420.
(44) Rappsilber, J. (2011) The beginning of a beautiful friendship: Cross-linking/mass spectrometry and modelling of proteins and multi-protein complexes. *J. Struct. Biol. 173*, 530−540.
(45) Petrotchenko, E. V., and Borchers, C. H. (2010) Crosslinking Combined with Mass Spectrometry for Structural Proteomics. *Mass Spectrom. Rev. 29*, 862−876.
(46) Kalkhof, S., Haehn, S., Paulsson, M., Smyth, N., Meiler, J., and Sinz, A. (2010) Computational modeling of laminin N-terminal domains using sparse distance constraints from disulfide bonds and chemical cross-linking. *Proteins 78*, 3409−3427.
(47) Hussain, S.-A., Carafoli, F., and Hohenester, E. (2011) Determinants of laminin polymerization revealed by the structure of the α5 chain amino-terminal region. *EMBO Rep. 12*, 276−282.
(48) Chen, Z. A., Jawhari, A., Fischer, L., Buchen, C., Tahir, S., Kamenski, T., Rasmussen, M., Lariviere, L., Bukowski-Wills, J. C., Nilges, M., Cramer, P., and Rappsilber, J. (2010) Architecture of the RNA polymerase II-TFIIF complex revealed by cross-linking and mass spectrometry. *EMBO J. 29*, 717−726.
(49) Dimova, K., Kalkhof, S., Pottratz, I., Ihling, C., Rodriguez-Castaneda, F., Liepold, T., Griesinger, C., Brose, N., Sinz, A., and Jahn, O. (2009) Structural Insights into the Calmodulin-Munc13 Interaction Obtained by Cross-Linking and Mass Spectrometry. *Biochemistry 48*, 5908−5921.
(50) Candiano, G., Bruschi, M., Musante, L., Santucci, L., Ghiggeri, G. M., Carnemolla, B., Orecchia, P., Zardi, L., and Righetti, P. G. (2004) Blue silver: A very sensitive colloidal Coomassie G-250 staining for proteome analysis. *Electrophoresis 25*, 1327−1333.
(51) Jensen, O. N., Shevchenko, A., and Mann, M. (1997) in *Protein Structure, a Practical Approach* (Creighton, T. E., Ed.) p 48, Oxford University Press, Oxford, U.K.
(52) Shevchenko, A., Tomas, H., Havlis, J., Olsen, J. V., and Mann, M. (2006) In-gel digestion for mass spectrometric characterization of proteins and proteomes. *Nat. Protoc. 1*, 2856−2860.
(53) Götze, M., Pettelkau, J., Schaks, S., Bosse, K., Ihling, C., Krauth, F., Fritzsche, R., Kühn, U., and Sinz, A. (2012) StavroX: A Software for Analyzing Crosslinked Products in Protein Interaction Studies. *J. Am. Soc. Mass Spectrom. 23*, 76−87.
(54) Kalkhof, S., and Sinz, A. (2008) Chances and pitfalls of chemical cross-linking with amine-reactive N-hydroxysuccinimide esters. *Anal. Bioanal. Chem. 392*, 305−312.
(55) Phillips, J. C., Braun, R., Wang, W., Gumbart, J., Tajkhorshid, E., Villa, E., Chipot, C., Skeel, R. D., Kale, L., and Schulten, K. (2005) Scalable molecular dynamics with NAMD. *J. Comput. Chem. 26*, 1781−1802.
(56) MacKerell, A. D., Bashford, D., Bellott, M., Dunbrack, R. L., Evanseck, J. D., Field, M. J., Fischer, S., Gao, J., Guo, H., Ha, S., Joseph-McCarthy, D., Kuchnir, L., Kuczera, K., Lau, F. T. K., Mattos, C., Michnick, S., Ngo, T., Nguyen, D. T., Prodhom, B., Reiher, W. E., Roux, B., Schlenkrich, M., Smith, J. C., Stote, R., Straub, J., Watanabe, M., Wiorkiewicz-Kuczera, J., Yin, D., and Karplus, M. (1998) All-atom

empirical potential for molecular modeling and dynamics studies of proteins. *J. Phys. Chem. B 102*, 3586−3616.
(57) Essmann, U., Perera, L., Berkowitz, M. L., Darden, T., Lee, H., and Pedersen, L. G. (1995) A Smooth Particle Mesh Ewald Method. *J. Chem. Phys. 103*, 8577−8593.
(58) Ryckaert, J. P., Ciccotti, G., and Berendsen, H. J. C. (1977) Numerical Integration of Cartesian Equations of Motion of a System with Constraints: Molecular Dynamics of N-Alkanes. *J. Comput. Phys. 23*, 327−341.
(59) Martyna, G. J., Tobias, D. J., and Klein, M. L. (1994) Constant-Pressure Molecular-Dynamics Algorithms. *J. Chem. Phys. 101*, 4177−4189.
(60) Feller, S. E., Zhang, Y. H., Pastor, R. W., and Brooks, B. R. (1995) Constant-Pressure Molecular-Dynamics Simulation: The Langevin Piston Method. *J. Chem. Phys. 103*, 4613−4621.
(61) Mädler, S., Bich, C., Touboul, D., and Zenobi, R. (2009) Chemical cross-linking with NHS esters: A systematic study on amino acid reactivities. *J. Mass Spectrom. 44*, 694−706.
(62) Suchanek, M., Radzikowska, A., and Thiele, C. (2005) Photo-leucine and photo-methionine allow identification of protein-protein interactions in living cells. *Nat. Methods 2*, 261−267.
(63) Humphrey, W., Dalke, A., and Schulten, K. (1996) VMD: Visual molecular dynamics. *J. Mol. Graphics 14*, 27−38.